

Department of Physics, Chemistry and Biology

Master's Thesis

# Search for Dark Matter in the Upgraded High Luminosity LHC at CERN

## Impact of ATLAS phase II performance on a mono-jet analysis

**Sven-Patrik Hallsjö**

Thesis work performed at Stockholm University

Linköping, June 4, 2014

LITH-IFM-A-EX--14/2863--SE



**Linköpings universitet  
TEKNISKA HÖGSKOLAN**

Department of Physics, Chemistry and Biology  
Linköping University  
SE-581 83 Linköping, Sweden



# **Search for Dark Matter in the Upgraded High Luminosity LHC at CERN**

## **Impact of ATLAS phase II performance on a mono-jet analysis**

**Sven-Patrik Hallsjö**

Thesis work performed at Stockholm University

Linköping, June 4, 2014

Supervisor:      **Docent Christophe Clément**  
                          FYSIKUM Stockholm University  
**Professor Magnus Johansson**  
                          IFM, Linköping University

Examiner:        **Professor Magnus Johansson**  
                          IFM, Linköping University





**Avdelning, Institution**  
Division, Department

Theoretical physics group  
Department of Physics, Chemistry and Biology  
SE-581 83 Linköping

**Datum**  
Date

2014-06-04

**Språk**  
Language

Svenska/Swedish  
 Engelska/English  
 \_\_\_\_\_

**Rapporttyp**  
Report category

Licentiatavhandling  
 Examensarbete  
 C-uppsats  
 D-uppsats  
 Övrig rapport  
 \_\_\_\_\_

**ISBN**  
—

**ISRN**  
LITH-IFM-A-EX--14/2863--SE

**Serietitel och serienummer**      **ISSN**  
Title of series, numbering      —

**URL för elektronisk version**

<http://urn.kb.se/resolve?urn=urn:nbn:se:liu:diva-XXXXX>

**Titel**      Sökandet efter mörk materia i den uppgraderade hög luminositets LHC i CERN  
Title      Search for Dark Matter in the Upgraded High Luminosity LHC at CERN

**Undertitel**      Påverkan av ATLAS fas II prestanda på en mono-jet analys  
Subtitle      Impact of ATLAS phase II performance on a mono-jet analysis

**Författare**      Sven-Patrik Hallsjö  
Author

**Sammanfattning**  
Abstract

Something as an introduction:

The LHC at CERN is undergoing an upgrade to increase the center of mass energy for the colliding particles which means that new physical processes will be explored. One drawback of this is that it will be harder to isolate unique particle collisions since more and more collisions will occur simultaneously, so called pile-up.

One hope for the upgrade is that WIMP models of dark matter will be detected.

This thesis covers looking at effective operators which try to explain dark matter without adding new theories to the standard model or QFT.

Some results and a slight conclusion.

**Nyckelord**

**Keywords**      ATLAS, Beyond standard model physics, CERN, Dark matter, Elementary particle physics, High energy physics, something, this is in mythesis.sty



## **4 Abstract**

**5 Something as an introduction:**

**6 The LHC at CERN is undergoing an upgrade to increase the center of mass en-**  
**7 ergy for the colliding particles which means that new physical processes will be**  
**8 explored. One drawback of this is that it will be harder to isolate unique parti-**  
**9 cle collisions since more and more collisions will occur simultaneously, so called**  
**10 pile-up.**

**11 One hope for the upgrade is that WIMP models of dark matter will be detected.**

**12 This thesis covers looking at effective operators which try to explain dark matter**  
**13 without adding new theories to the standard model or QFT.**

**14 Some results and a slight conclusion.**



<sup>15</sup> **Acknowledgments**

<sup>16</sup> I wish to dedicate this thesis to my mathematics teacher Ulf Rydmark without  
<sup>17</sup> whom I would not have studied physics.

<sup>18</sup> A big thank you to my family, fiancée and friends who have supported me through-  
<sup>19</sup> out my education. A warm thank you to my friend Joakim Skoog who altered  
<sup>20</sup> some of the images for me.

<sup>21</sup> I want to thank my supervisor Christophe Clément and all those who helped me  
<sup>22</sup> at Stockholm University.

<sup>23</sup> I also want to thank my examiner Magnus Johansson, who always took time to  
<sup>24</sup> answer any question from and support his students.

<sup>25</sup> A special thank you to Professor Irina Yakimenko without whom my master years  
<sup>26</sup> would have been duller and probably impossible.

<sup>27</sup> Finally I want to thank someone someone for proofreading my

*Linköping, June 2014*  
*Sven-Patrik Hallsjö*



---

# Contents

## Notation

### 1 Introduction

1.1	Research goals . . . . .	2
1.2	Theoretical Background . . . . .	3
1.2.1	Quantum mechanics and quantum field theory . . . . .	3
1.2.2	Nuclear, particle and subatomic particle physics . . . . .	4
1.2.3	The standard model of particle physics . . . . .	4
1.2.4	Dark matter . . . . .	5
1.2.5	Effective field theory . . . . .	6
1.2.6	Search for WIMPS . . . . .	8
1.3	Experimental overview . . . . .	10
1.3.1	LHC . . . . .	10
1.3.2	ATLAS . . . . .	11
1.3.3	Coordinate system . . . . .	12
1.3.4	Reconstructing data . . . . .	12
1.3.5	Pile-up . . . . .	13
1.3.6	Mono-jet analysis . . . . .	13
1.3.7	Phase II high luminosity upgrade . . . . .	14
1.3.8	Monte Carlo simulation . . . . .	15

### 2 Validation of smearing functions

2.1	Smearing functions . . . . .	18
2.2	Validation . . . . .	19
2.3	Results . . . . .	20
2.3.1	Electron and photon . . . . .	21
2.3.2	Muon . . . . .	22
2.3.3	Tau . . . . .	22
2.3.4	Jets . . . . .	23
2.3.5	Missing Transversal Energy . . . . .	24
2.4	Expected results . . . . .	25
2.5	Discussion . . . . .	27
2.5.1	Smearing independent on pile-up . . . . .	27

63	2.5.2 Comparison to expected results . . . . .	27
64	2.6 Conclusion . . . . .	28
65	<b>3 Evaluating dark matter signals</b>	<b>29</b>
66	3.1 Signal to background ratio . . . . .	29
67	3.1.1 Selection criteria . . . . .	30
68	3.1.2 Verifying background data . . . . .	30
69	3.1.3 Figures of merit . . . . .	31
70	3.1.4 D5 operators . . . . .	32
71	3.1.5 Light vector mediator models . . . . .	32
72	3.1.6 Susy models? . . . . .	32
73	3.2 Other selection criteria and observables . . . . .	32
74	3.3 Mitigating the effect of the high luminosity . . . . .	32
75	3.4 Results . . . . .	33
76	3.4.1 Limit on $M^*$ . . . . .	33
77	3.4.2 Effect of pile-up on $M^*$ . . . . .	33
78	3.4.3 Previous results . . . . .	34
79	3.4.4 Limit on mediator mass . . . . .	34
80	3.4.5 Effect of pile-up on mediator mass . . . . .	34
81	3.5 Discussion . . . . .	34
82	3.6 Conclusion . . . . .	34
83	<b>4 Results and Conclusions</b>	<b>35</b>
84	4.1 Validation of smearing functions . . . . .	35
85	4.2 Signal to background ratio . . . . .	35
86	4.2.1 Limit on $M^*$ . . . . .	35
87	4.2.2 Limit on mediator mass . . . . .	35
88	4.3 Other selection criteria and observables . . . . .	35
89	4.3.1 Limit on $M^*$ . . . . .	35
90	4.3.2 Limit on mediator mass . . . . .	35
91	4.4 Mitigating the effect of the high luminosity . . . . .	35
92	4.5 Recommendations to mitigate the effect of the high luminosity . . . . .	35
93	4.6 Suggestions for future research . . . . .	36
94	<b>A Datasets</b>	<b>39</b>
95	A.1 Background processes . . . . .	39
96	A.1.1 Validation . . . . .	39
97	A.1.2 Background to signals . . . . .	39
98	A.2 D5 signal processes . . . . .	40
99	A.3 Light vector mediator processes . . . . .	40
100	<b>Bibliography</b>	<b>45</b>

# Notation

## NOTATIONS

Notation	Explanation
barn(b)	1 barn(b)= $10^{-24}$ cm <sup>2</sup>
$\oplus$	$a \oplus b = \sqrt{a^2 + b^2}$ , $a \oplus b \oplus c = \sqrt{a^2 + b^2 + c^2}$

## ABBREVIATIONS

Abbreviation	Expansion
ATLAS	A large Toroidal LHC ApparatuS
CERN	Organisation européenne pour la recherche nucléaire <sup>1</sup>
CMS	Compact Muon Solenoid
LHC	Large Hadron Collider
RMS	Root Mean Square
SM	the Standard Model of particle physics
WIMP	Weakly Interacting Massive Particle
WIMPS	Weakly Interacting Massive ParticleS
QED	Quantum ElectroDynamics
QFT	Quantum Field Theory
QM	Quantum Mechanics

<sup>1</sup>Originally, Conseil Européen pour la Recherche Nucléaire



# 1

---

## Introduction

107 Discrepancies in measurements of the rotations of galaxies indicate the presence  
108 of a large amount of matter which interacts through gravity, though not elec-  
109 tromagnetically making it invisible to our telescopes. This matter is commonly  
110 referred to as dark matter. Since no known or hypothesised particle in the stan-  
111 dard model of particle physics can be used as a candidate for dark matter, this  
112 hints at the presence of new physics.

113 At the Organisation Européene pour la Recherche Nucléaire (CERN) focus now  
114 lies to discover any evidence of so called weakly interacting massive particles  
115 (WIMPS) which may be a candidate for dark matter. It is usually impossible to  
116 detect any interaction of dark matter candidates on the subatomic scale, however  
117 through looking at proposed interactions, searching for assumed decay channels  
118 and by investigating what is invisible to the detectors by using momentum con-  
119 servation it is hoped that signs will be found. Though to date, none have been  
120 found.

121 Both experiments and current theories now show that higher energies are re-  
122 quired at the LHC to be able to see any signs. This is why the LHC and all detectors  
123 are undergoing a vast upgrade program [1]. In this thesis focus will be on the last  
124 part of the upgrade due for completion in 2023, known as the high luminosity-  
125 LHC phase II upgrade; and also on the ATLAS detector. The method used in this  
126 thesis focuses on looking at data which emulate conditions at the upgraded LHC.

## 127 1.1 Research goals

128 This research took place at Stockholm University from January 7th until **when**?  
129 During the research period the following tasks were set up and performed/answered:

- 130 • Implement a C++ programme that loops over the collisions inside the signal  
131 and background datasets.
- 132 • For each collision retrieve the relevant observables (variables used to extract  
133 the signal over the background) and apply "smearing functions" to emulate  
134 the effect of the high luminosity on the observables.
- 135 • For both signal and background datasets, compare observables before and  
136 after smearing. What observables are the least/most affected?
- 137 • Implement selection criteria that selects the signal collisions efficiently while  
138 reduces significantly the background. In a first step the selection criteria  
139 should be taken from existing studies.
- 140 • Selection criteria can be evaluated and compared with each other using a  
141 figure of merit  $P$ , that measures the sensitivity of the experiment to the dark  
142 matter signal. Calculate  $P$  for the given selection criteria before and after  
143 smearing.
- 144 • What is the effect of the high luminosity (smearing) on the value of  $P$ ?
- 145 • Investigate other selection criteria and observables, to mitigate the effect of  
146 high luminosity. Use  $P$  to rank different criteria after smearing.
- 147 • Conclude on the effect of the high luminosity on the sensitivity for dark matter  
148 and possible ways to mitigate its effects using alternative observables  
149 and selection criteria.

## 1.2 Theoretical Background

### 1.2.1 Quantum mechanics and quantum field theory

In the beginning of the 20th century, some physical phenomena could not be explained by classical physics, for example the ultra-violet disaster of any classical model of black-body radiation, and the photoelectric effect [2]. It was these phenomena that led to the formulation of quantum mechanics (QM), where energy transfer is quantized and particles can act as both waves and particles at the same time [3].

Combining QM with classical electromagnetism proved harder than expected, colliding a photon(em-field) and an electron (particle/wave) is quite tricky. This can be seen when trying to calculate the scattering between them both in a QM schema. One idea that came from this was to explain them both in the same framework, field theory. Also, trying to incorporate special relativity into QM suggested a field description where space-time is described using the metric formalism from differential geometry. The culmination of both of these problems is the first part of a Quantum field theory (QFT), Quantum electrodynamics (QED) which with incredible precision explains electromagnetic phenomena including effects from special relativity[4]. It is in this merging that antimatter was theorised, since it is a requirement for the theory to hold. After the discovery of antimatter, the theory was set in stone. Since this the theory has been altered somewhat to explain more and more experimental data. This is discussed more in subsection 1.2.2 and subsection 1.2.3.

To be able to calculate properties in QFT one uses the Lagrangian formalism [5], which gives a governing equation for the different physical processes. In general the Lagrangian used for the Standard model is quite complicated, one can thus focus on one of the different terms corresponding to a specific interaction. This can be done to calculate the so called cross-section for a process, which is related to the probability that that process will occur. A step to simplify the calculations is to use the so called Feynman diagrams, an example of which is given in figure 1.1.

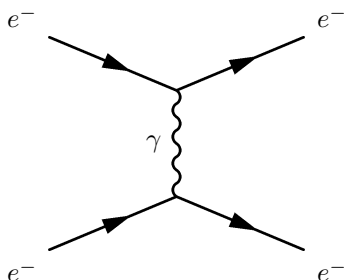


**Figure 1.1:** An example of a Feynman diagram explaining an electron-electron scattering using QED.

Through the figure, which comes with certain rules, and knowing what the major process (in this case QED) one can calculate the cross-section [4]. It is this that is needed to predict what one will be able to detect new particles.

## 1.2.2 Nuclear, particle and subatomic particle physics

Many could argue that these branches of physics started after Ernest Rutherford famous gold foil experiment [6], where he discovered that matter is composed of matter with a nucleus, a lot of empty space and electrons.

It was this that sparked the curiosity to see what the nucleus is made of and what forces govern the insides of atoms. After this, and the combination of the theoretical description given by QM, a lot more has been discovered and still more has been predicted. The newest of these is of course the Higgs particle, which was predicted through QFT and then discovered by the ATLAS and the CMS experiments at CERN [7].

The discovered particles are often divided into different groups depending on the fundamental particles that build them up. For instance, particles build up of three quarks are known as hadrons. Particles with an integer spin are known as bosons whereas half-integer particles are known as fermions.

## 1.2.3 The standard model of particle physics

The standard model of particle physics, referred to simply as the standard model (SM), is the particle zoo which tries to categorize all the particles and that have been discovered experimentally. QFT explains the interactions between these particles and it has also predicted several particles by including symmetries [6]. Regarding SM, Gauge bosons are the force carriers for the different forces, quarks are the and leptons are the fundamental blocks that we know of so far. The difference between the later two is if they interact via the strong force or not.

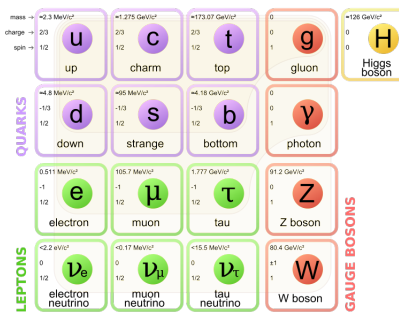


**Figure 1.2:** The standard model of particle physics where the three first columns represent the so called generations, starting with the first. [8].

SM is today the pinnacle of particle physics and can be used to explain almost everything that occurs around us. There are however some problems [9]:

- No QFT for general relativity! There is no link between gravity and the SM.
- Asymmetry between matter and antimatter can not be fully explained.
- No dark matter candidate!
- No explanation that can contain dark matter.

211 In this thesis focus lies with dark matter, some more introduction to possible  
 212 dark matter and different candidates in extensions to SM are explained in subsec-  
 213 tion 1.2.4.

### 214 1.2.4 Dark matter

215 Dark matter is among other things, the name given to the solution to the discrep-  
 216 ancies of galactic rotations.

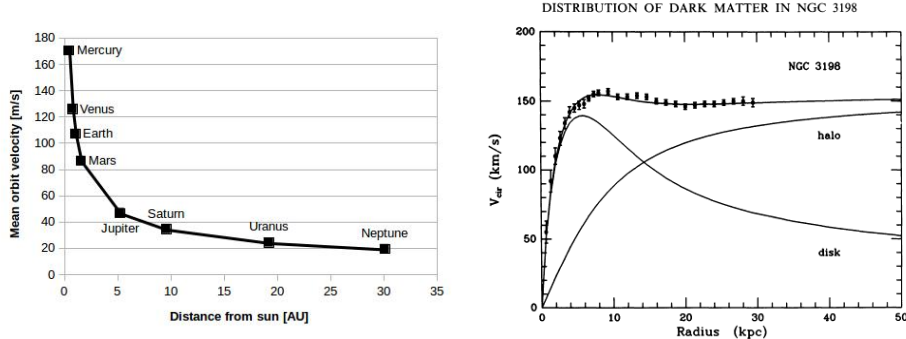
217 To explain this, focus on matter in a galaxy which are rotating around the center  
 218 of the galaxy. Through Newtons law of gravity and the centrifugal force one can  
 219 calculate the rotation speed dependent on the distance to the center of the galaxy.  
 220 Since one of these forces is attractive and the other repulsive, if the matter is in  
 221 a stable orbit around the galactic center (which they are) they must be equal and  
 222 give us an expression for the speed depending on the distance. Newtons law can  
 223 be written as the following:

$$F_{Gravitational} = G \frac{Mm}{r^2} = G_M \frac{m}{r^2} \quad F_{Centrifugal} = m \frac{V^2}{r} \quad (1.1)$$

224 where G is the gravitational constant, M the mass of the centre object, m the mass  
 225 of the matter, r the distance between the two and V is the rotation speed. It has  
 226 been simplified using  $G_M$  since all matter orbits the same galactic center. Setting  
 227 the equations in (1.1) results in:

$$G_M \frac{m}{r^2} = m \frac{V^2}{r} \Leftrightarrow V^2 = \frac{G_M}{r} \Rightarrow V = \sqrt{\frac{G_M}{r}} \propto \frac{1}{\sqrt{r}} \quad (1.2)$$

228 where the speed is assumed to be positive and  $\propto$  means proportional. Through  
 229 these simple calculations it shown that the rotation speed should decrease with  
 230 and increased distance. The same reasoning can be applied to our solar system  
 231 where this is the case figure 1.3a. The relation in these units is  $V = \frac{107}{\sqrt{r}}$  where  
 232 107 can be used in (1.2) to calculate the mass of the sun. However when looking  
 233 at galaxies, even when taking into account that one has to see the galaxies as a  
 234 mass distribution and that the above is only true when outside of the inner mass  
 235 half, this is not the case! In figure 1.3b experimental data can be seen from the  
 236 galaxy NGC3198 with a fitted curve which does not decrease with the distance  
 237 but is instead constant. This is the discrepancy which is solved by postulating  
 238 the existence of dark matter. After this the big question arises, what could this  
 239 dark matter consist of? What is known so far lies in the name. It is called dark  
 240 since no electromagnetic interaction and matter since gravitational interaction.  
 241 This means that it can not be made up of any baryonic matter or anything in  
 242 the Standard Model apart from neutrinos. The main interest of this thesis and  
 243 also the main contributor to the rotational discrepancies is known as cold dark  
 244 matter. This is due to the matter having a low speed, thus low kinetic energy, and  
 245 have a high particle mass (In the GeV scale) [9, 12, 13]. This means however that  
 246 neutrinos can not be a candidate, thus dark matter can not be made out of any  
 247 standard model particles. There are several ideas to detected dark matter, [9]



(a) Rotation speed of planets in our solar system. Since the distance is quite small on an astronomical scale, there is no sign of dark matter. Based on data from [10].

(b) Rotation speed of matter in NGC3198 with a curve fitting and three different models, if only a dark model halo existed, if there was no dark matter and the correct, if both exist [11].

**Figure 1.3:** Different rotation curves, both for planets in our solar system and matter in the NGC3198 galaxy.

- Ordinary matter interacting with ordinary matter can produce dark matter, known as production. Which is the processes that occurs at particle accelerators.
- Dark matter interacting with ordinary matter can produce dark matter, known as direct detection.
- Dark matter interacting with dark matter can produce ordinary matter, known as indirect detection.

In this thesis the focus lies with production. There are several theories how to detect dark matter in proton-proton collisions such that occur at the LHC at CERN this is covered more in subsection 1.2.6.

## 1.2.5 Effective field theory

In quantum field theory the objective is usually to find the part of the Lagrangian which explains a type of interaction, known as the operator of the interaction and also to find the probability amplitude (cross-section) for a certain interaction. For complicated processes it is easier to employ certain conditions so that the small scale phenomena are simplified and the whole picture understood. This is known as using an effective field theory and the idea can be seen in figure 1.4. The operator can be found through assuming the possible interactions and using the effective field theory [4]. The cross-sections can be found through the Feynman diagrams as described in subsection 1.2.1.

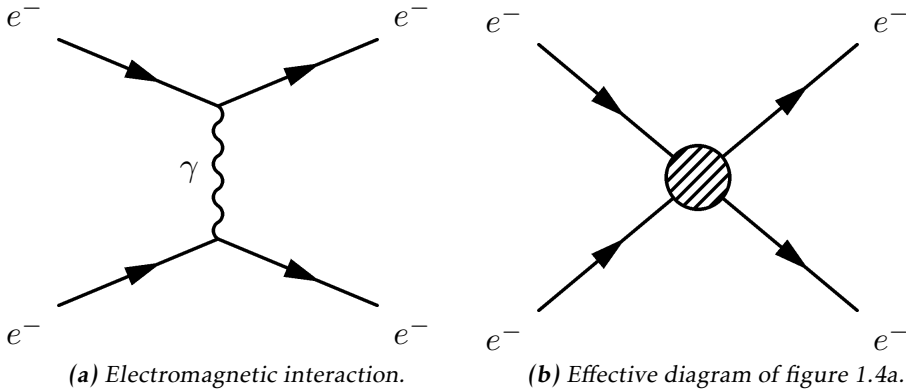


**Figure 1.4:** Feynman diagram of an electron-electron scattering, both as an ordinary diagram and as its effective theory version, where the details are hidden in the blob.

In this thesis the same effective field theory as in Refs. [12, 14] will be considered. The WIMP (usually denoted  $\chi$ ) is assumed to be the only particle in addition to the standard model fields.  $\chi$  will be assumed odd under some  $Z_2$  symmetry. This means that an even number of  $\chi$  must be in every coupling. It is assumed that the whatever mediator exists is heavier than the WIMPS, meaning that their interactions are in higher order terms of the effective field theory and thus not included in the operators. For simplicity, the WIMPS are assumed to be SM singlets, thus invariant under SM gauge transformations, and the coupling to the Higgs boson is neglected.

The focus for the operators will be quark bilinear operators on the form  $\bar{q}\Gamma q$  where  $\Gamma$  is a  $4 \times 4$  matrix of the complete set,

$$\Gamma = \{1, \gamma^5, \gamma^\mu, \gamma^\mu \gamma^5, \sigma^{\mu\nu}\} \quad (1.3)$$

279 This will dictate how the operators are written, more of why this is done can be  
280 found in [4, 12, 14].

281 This, together with the coupling with the strong force defines an effective field  
 282 theory of the interaction of singlet WIMPs with hadronic matter. It is a non-  
 283 renormalizable field theory which will break down when the mediator mass is  
 284 close to the mass of the WIMP. The condition for this is derived in [14] and gives:

$$M > 2m_\chi \quad (1.4)$$

where  $m_\chi$  is the mass of the WIMP and  $M$  is the mass of the mediator. There is also the requirement that:

$$M \lesssim 4\pi M_* \quad (1.5)$$

<sup>287</sup> where  $M_*$  is the energy scale where the effective theory is no longer a good ap-

288 proximation.

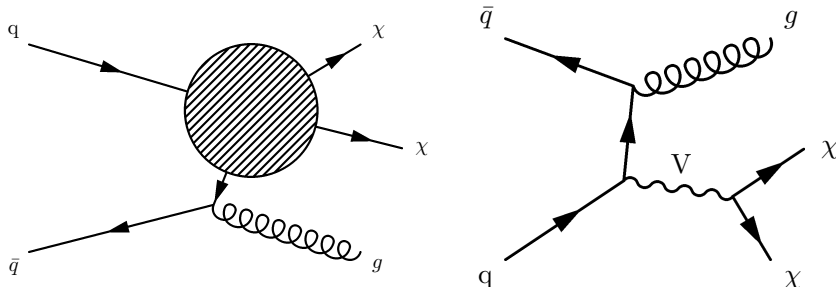
289 In this work, WIMPS are assumed to be Dirac fermions (half integer spin and is  
290 not its own antiparticle).

291 In table 1.1 the operators which are integrated out via the effective field theory  
292 and are of interest in this thesis are given.

Name	Initial state	Type	Operator
D1	qq	scalar	$\frac{m_q}{M_*^3} \bar{\chi} \chi \bar{q} q$
D5	qq	vector	$\frac{1}{M_*^2} \bar{\chi} \gamma^\mu \chi \bar{q} \gamma_\mu q$
D8	qq	axial-vector	$\frac{1}{M_*^2} \bar{\chi} \gamma^\mu \gamma^5 \chi \bar{q} \gamma_\mu \gamma^5 q$
D9	qq	tensor	$\frac{1}{M_*^2} \bar{\chi} \sigma^{\mu\nu} \chi \bar{q} \sigma_{\mu\nu} q$
D11	gg	scalar	$\frac{1}{4M_*^3} \bar{\chi} \chi \alpha_s (G_{\mu\nu}^a)^2$

**Table 1.1:** Table based on discussion in [13]

293 Where D denotes that the WIMPS are assumed to be Dirac fermions. These can all  
294 be described using figure 1.5a



**(a)** Effective Feynman diagram explaining the D-operators.

**(b)** Feynman diagram describing the vector mediator model.

**Figure 1.5:** Feynman diagrams describing the used signal models.

295 Another model which is considered is when the WIMP mass is close to the me-  
296 diator mass. Then the effective theory fails and the process is assumed to be  
297 described by figure 1.5b.

## 298 1.2.6 Search for WIMPs

299 The search of WIMPS is based on a mono-jet analysis which is described in sub-  
300 section 1.3.6. This method revolves around looking at all energy before and after

301 a collision and making sure energy conservation exists. If it does not, then some-  
302 thing has happened which the detectors can not detect. If it is so that the models  
303 from subsection 1.2.5 can explain the missing energy, then a model for WIMPS  
304 has been found.

305 Since the search for WIMPS at the LHC is based on looking at the missing energy,  
306 not actual detection, the experiment can not establish if a WIMP is stable on a  
307 cosmological time scale and thus if it is a dark matter candidate [13]. This means  
308 that if a candidate is found, it may still not be the dark matter that is needed to  
309 explain the cosmological observations.

310 The different theories discussed in subsection 1.2.5 requires some process in  
311 which quarks and anti-quarks are produced. This process happens in a lot of  
312 different accelerators. The main problem is that nothing has been found low en-  
313 ergy levels. This is why it is very interesting that the LHC is undergoing a upgrade  
314 that will allow higher energy levels, see subsection 1.3.7. With this the processes  
315 can be given higher energy and thus the produced particles can be comprised of  
316 higher mass.

## 317 1.3 Experimental overview

### 318 1.3.1 LHC

319 The Large hadron collider (LHC) is a particle accelerator located at CERN near  
 320 Geneva in Switzerland, see figure 1.6. The accelerator was built to explore physics  
 321 beyond the standard model and to make more accurate measurements of stan-  
 322 dard model physics. Before it was shut down for an upgrade in 2012 it was able  
 323 to accelerate two proton beams to such a velocity that they had an energy of 4 TeV  
 324 which gives a center of mass energy,  $\sqrt{s} = 8$  TeV. It should be noted that the pro-  
 325 ton beam is not homogeneous, it is comprised of bunches of protons with enough  
 326 spacing that bunch collisions can happen independent of each other. Apart from  
 327 the energy, the ability for an accelerator to produce interactions can be calculated  
 328 through the instantaneous luminosity of the LHC was  $10^{34} \text{ cm}^{-2}\text{s}^{-1}$  or  $10\text{nb}^{-1}\text{s}^{-1}$   
 329 where 1 barn(b)=  $10^{-24} \text{ cm}^2$ . All values taken from [15].

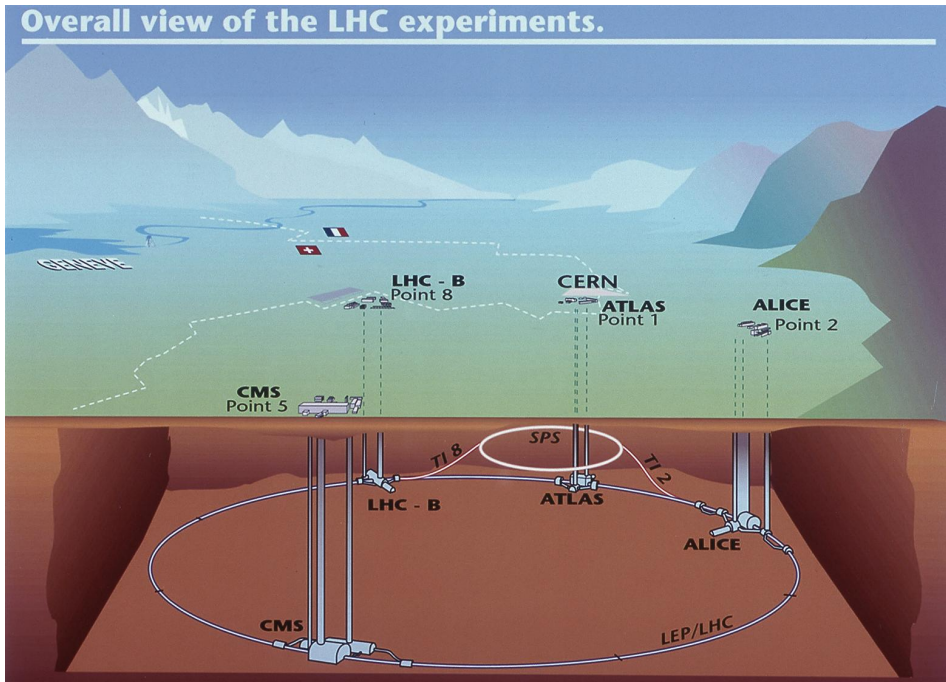


Figure 1.6: Figure showing the LHC and the different detector sites[16]

330 The instantaneous luminosity, often just denoted luminosity, can be defined in  
 331 different ways depending on how the collision takes place. For two collinear  
 332 intersecting particle beams it is defined as:

$$\mathcal{L} = \frac{f k N_1 N_2}{4\pi \sigma_x \sigma_y} \quad (1.6)$$

333 where  $N_i$  are the number of particles in each of the bunches,  $f$  is the frequency  
 334 at which the bunches collide ,  $k$  the number of colliding bunches in each beam,  
 335 and  $\sigma_x$  ( $\sigma_y$ ) is the horizontal (vertical) beam size at the interaction point. Since  
 336 the instantaneous luminosity increases quadratically with more particles in each  
 337 bunch this would be a good strategy. However aside from the difficulties to create  
 338 and maintain a beam with more particles, a large  $N_i$  increases the probability for  
 339 multiple collisions per bunch crossing, referred to as pile-up. Pile up will be a  
 340 key aspect which is described more in subsection 1.3.5.

341 The expected number of events can be calculated by using the instantaneous lu-  
 342 minosity through the following:

$$N = \sigma \int \mathcal{L} dt := \sigma \mathcal{L} \quad (1.7)$$

343 where  $\mathcal{L}$  is the integrated luminosity and  $\sigma$  is the cross section which is often  
 344 measured in barn. The integrated luminosity is a measurement of total number  
 345 of interactions that have occurred over time. Before the LHC was shut down this  
 346 values was  $20.8 \text{ fb}^{-1}$ .

347 The cross section is defined through the integral of the differential cross section,  
 348 as explained in subsection 1.2.1, over the whole solid angle:

$$\sigma = \oint d\Omega \frac{d\sigma}{d\Omega} \quad (1.8)$$

349 The cross section is therefore a measure of the effective surface area seen by the  
 350 impinging particles, and as such is expressed in units of area. The cross section  
 351 is proportional to the probability that an interaction will occur. It also provides a  
 352 measure of the strength of the interaction between the scattered particle and the  
 353 scattering center. Further details can be found in reference [17]

### 354 1.3.2 ATLAS

355 As seen in figure 1.6, there are several detectors at CERN. One of these is a large  
 356 toroidal LHC apparatus (ATLAS) which is a general purpose detector that uses  
 357 a toroid magnet. Its goal is to observe several different production and decay  
 358 channels. The detector is composed of three concentric sub-detectors, the Inner  
 359 detector, the Calorimeters and the Muon spectrometer [18].

360 The Inner detectors main job is to detect the tracks of the particles and their  
 361 interaction with the material in the detector.

362 The Calorimeters, the electromagnetic and hadronic, are used to calculate the  
 363 energy contained in the different particles (**electromagnetic get this and that,**  
 364 **hadronic get this and that**).

365 The Muon spectrometer is used to detect signs of muons, which will simply pass  
 366 through the other detectors without leaving a trace.

367 From this, it is known that neutrinos, and as assumed in this thesis WIMPS pass  
 368 through all the detectors without leaving a trace.

### 369 1.3.3 Coordinate system

370 The coordinate system of ATLAS, seen in figure 1.7 is a right-handed coordinate  
 371 system with the x-axis pointing towards the centre of the LHC tunnel, and the  
 372 z-axis along the tunnel/beam (counter clockwise) seen from above. The y-axis  
 373 points upward. The origin is define as the interaction point. A cylindrical coor-  
 374 dinate system is also used for the transversal plane. ( $R, \phi, Z$ ). For simplicity the  
 375 pseudorapidity of particles from the primary vertex is defined as:

$$\eta = -\ln(\tan \frac{\theta}{2}) \quad (1.9)$$

376 where  $\theta$  is the polar angle (xz-plane) of the particle direction measured from  
 377 the positive z-axis.  $\eta$  is through this definition invariant under boosts in the z-  
 378 direction.

379 It is quite common to calculate the distance between particles and jets in the  
 380  $(\eta, \phi)$  plane,  $d = \sqrt{(\Delta\eta)^2 + (\Delta\phi)^2}$

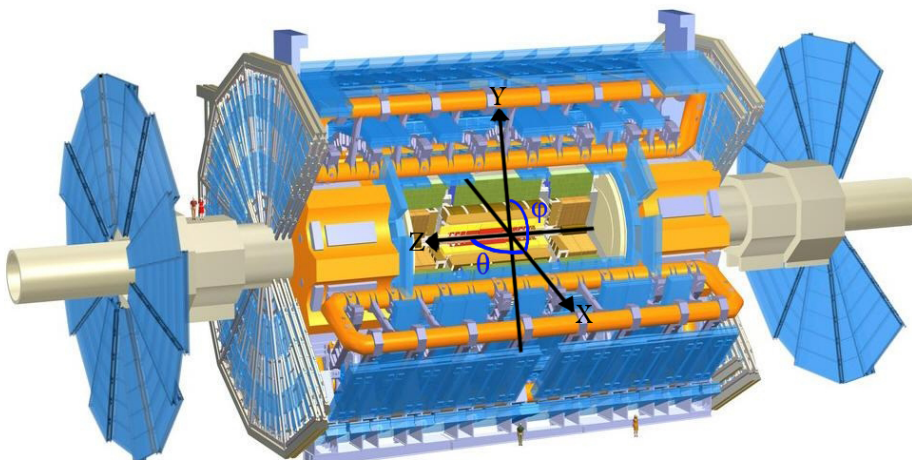


**Figure 1.7:** Figure showing the ATLAS detector and the definition of the orthogonal Cartesian coordinate system. Image altered from[19]

### 381 1.3.4 Reconstructing data

382 To be able to compare the emulated data to measurable data it is important to  
 383 include effects of the detectors. This is done using so called smearing functions  
 384 which try to emulate the reconstruction of data.

385 The reconstruction process of data [18], is based on what response is given from  
 386 the detectors. It is affected by pile-up and the energy of that which is detected.  
 387 The reconstruction process is not specifically used in the thesis, however the  
 388 smearing functions are discussed in section 2.1.

### 389 1.3.5 Pile-up

390 Pile-up is defined as the average number of proton-proton collisions that occur  
 391 per bunch crossing per second. It is denoted as  $\langle \mu \rangle$ .  $\mu$  can be calculated by adjust-  
 392 ing a Poisson distribution to fit the curve created by the number of interactions  
 393 per bunch crossing at a given luminosity. When this is done  $\mu$  will be the mean  
 394 value of the Poisson distribution.

### 395 1.3.6 Mono-jet analysis

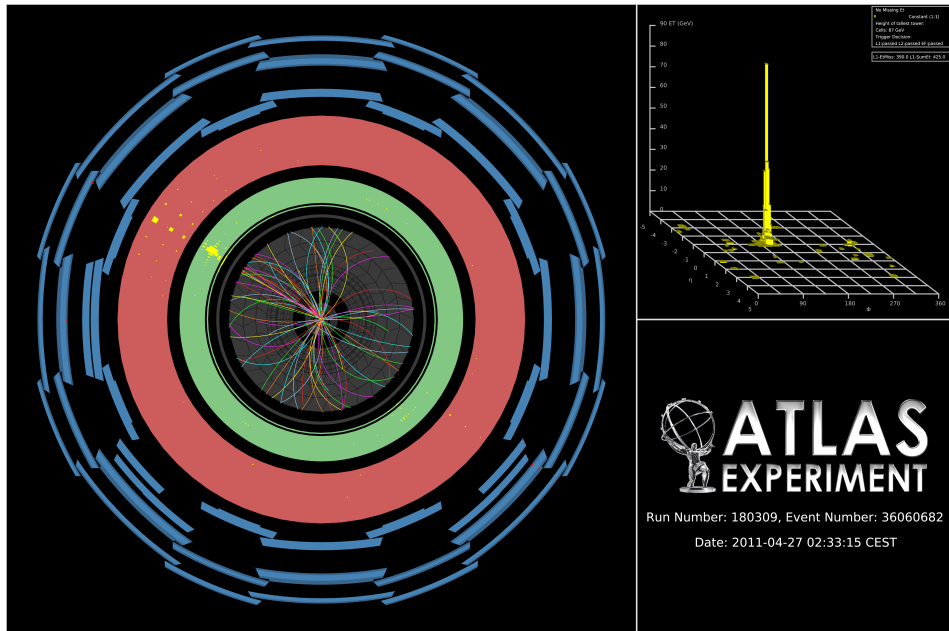


**Figure 1.8:** Image of a mono-jet event [20].

396 When measuring the transversal energy one can in some interactions find incon-  
 397 sistencies, such as jets that are in excess in one direction. In figure 1.8 one can see  
 398 a high energetic jet which gives an excess of transversal energy in one direction  
 399 after the collision. Since there is no balancing jet there must be transversal energy  
 400 that is not detected, denoted  $E_T^{Miss}$ , since it was close to zero before the collision.  
 401 This gives an indication that there energy to balance this that simply can not be  
 402 detected. This could for instance be neutrinos or the sign of a new particle.

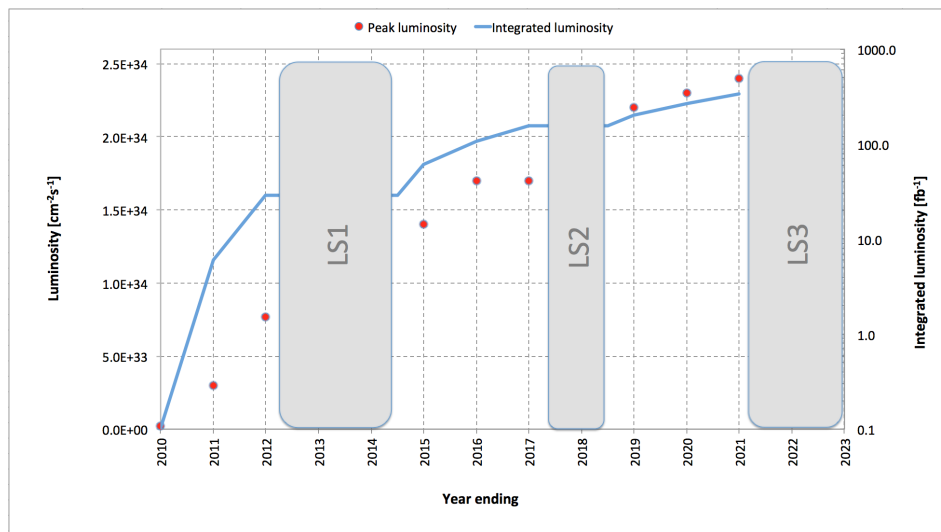
403 Jets are showers of particles that are produced at collisions. They are composed  
 404 of highly energetic quarks and/or gluons. Since the gluons have self interaction,  
 405 they split into even more gluons which then results in shower of particles mov-  
 406 ing in the same direction. In the final stages the quarks and gluons can combine  
 407 to form larger particles. It is by measuring these end products that one can gain  
 408 more information about the collision which created the jet.

409 There are two main concepts to the analysis, signal and background. The signal  
 410 is what theoretically should be detected by a assumed process. In this thesis the  
 411 different dark matter processes, from subsection 1.2.5, will constitute different  
 412 signals. However to know that the missing energy is sign of the signal then one  
 413 must understand all the other components that could contribute to the missing  
 414 energy.

415 The background comprises of all the background processes that occur and that  
 416 could contribute to the missing energy. By finding so called Control regions,  
 417 where background process are in excess, one can model the missing energy by  
 418 how many neutrinos come from the processes.

### 419 1.3.7 Phase II high luminosity upgrade

420 At the moment, the whole LHC is undergoing a huge upgrade program which be fi-  
 421 nished around 2022-2023, denoted the high luminosity upgrade, or HL-upgrade.  
 422 The upgrade contains of different stages, meaning that the upgrade will halt for  
 periods so that experiments can take place. In figure 1.9 one can see the three



423 **Figure 1.9:** A graph showing the upgrading timetable with the instantaneous  
 424 luminosity, denoted luminosity, and integrated luminosity expected in the  
 425 different stages.

426 proposed upgrades. LS1 is denoted phase 0, LS2 phase I and LS3 phase II.  
 427 LS1 is the upgrade which will take the LHC to its designed performance.  
 LS2 will take the LHC to the ultimate designed instantaneous luminosity.  
 LS3 which is the upgrade which is of focus in this thesis, will increase the instantaneous luminosity yet again. Though for this to happen a modification of

429 the whole LHC must be done, instead of just an upgrade and maintenance  
 430 as before.

- 431 The following is expected for the experiments done after phase II:

Entity	Expected	Last run (2012)
Instantaneous luminosity	$\mathcal{L} \sim 50 \text{ nb}^{-1}\text{s}^{-1}$	$\mathcal{L} \sim 10 \text{ nb}^{-1}\text{s}^{-1}$
Integrated luminosity	$\mathcal{L} = 1000 - 3000 \text{ fb}^{-1}$	$\mathcal{L} = 20 \text{ fb}^{-1}$
Pile-up	$\langle \mu \rangle = 140$	$\langle \mu \rangle = 20$
Center of mass energy	$\sqrt{s} = 14 \text{ TeV}$	$\sqrt{s} = 8 \text{ TeV}$

**Table 1.2:** Expected running values for the Phase II HL-upgraded LHC with older values for comparison [21].

432 Where it should be noted that the integrated luminosity indicates the total amount  
 433 of data which will be collected after the upgrade is completed before the next up-  
 434 grade takes place.

### 435 1.3.8 Monte Carlo simulation

436 As mentioned before, in this thesis only emulated data has been used. This data  
 437 is created by using a Monte Carlo simulation of the background processes and  
 438 the expected signal. To do this a program called MadGraph is used.

439 MadGraph [22] starts with Feynman diagrams and then generates simulated events  
 440 based on lots of different parameters. To create correct simulations for this anal-  
 441 ysis PYTHIA has been used.

442 PYTHIA [23] is a package which adds the correct description of jets and missing  
 443 energy to MadGraph. PYTHIA also adds the correct description of pile-up.

444 The tool to access all this data and analyse it a tool called ROOT was used. ROOT  
 445 is used for programming high energy physics related tools [24]



# 2

---

## Validation of smearing functions

448 One might assume that using a Monte Carlo simulation it would be easy to model  
449 and emulate the whole process, from collision to detection and reconstruction in  
450 the upgraded LHC. It is possible, but it requires a lot of computing power. Instead  
451 one can use one simulation and a mathematical model to calculate the estimated  
452 response in the detector. This was validated and used in this thesis to be able to  
453 create the data needed for further analysis.

454 This was done by using a Monte Carlo simulation of a proton-proton collision and  
455 applying the official Truth to reco code, also known as the smearing functions,  
456 that was developed using previous studies [1, 25]. to simulate how the detector  
457 and the reconstruction is affected by the increased luminosity and the pile-up  
458 that comes with this.

459 The code uses the experimental data from the previous studies to smear the re-  
460 constructed energy and momenta, it is from this that the name smearing func-  
461 tions comes. The key feature of those studies were that the direction of the mo-  
462 mента is unaffected and that only jets and  $E_T^{Miss}$  are affected by pile-up. This was  
463 confirmed in previous studies and were thus not incorporated into the smearing  
464 functions, more in section 2.1.

## 465 2.1 Smearing functions

466 **Put in introduction? The particles that are directly detectable in ATLAS are:**  
467 electron, photon, muon, tau. Aside from this jets can be detected, and from this  
468  $E_T^{Miss}$  can be calculated.

469 This means that the all detectable entities must have their own smearing func-  
470 tions.

471  $E_T^{Miss}$ , the missing transversal energy, which was discussed in subsection 1.3.6, is  
472 calculated by knowing that there should be energy conservation in the collision.  
473 It is comprised of different parts, one from neutrinos, one from errors in the  
474 other measurements and one from (hopefully) new physics.

475 The jet and  $E_T^{Miss}$  are the only "parts" which are not unique particles instead they  
476 are based either on a shower of particles or the energy which is missing from  
477 the conservation of transversal energy. Thus, the pile-up dependence here must  
478 simply come from the fact that it is hard to separate the different jets and that  
479 with several different collisions occurring makes it hard to accurately measure  
480 the total energy.

481 The electron and photon have the same smearing since they are both detected  
482 in a similar way. Perhaps add more to the introduction about each part of the  
483 detector. or simply write that here?

484 The muon is special since it is detected in the muon spectrometer.

485 Tau is detected similarly to electron and photon.

486 These smearing functions are designed so that they take into account the effi-  
487 ciency of the different detectors, limitations as well as their dependence on pile-  
488 up. They also take into account how all this varies depending on the measured  
489 entries energy or momenta.

490 The terminology is that data before smearing, simulated data, is denoted as data  
491 at a truth level or truth data. Data after smearing, which is comparable to what  
492 is measured, reconstructed or reco data as discussed in subsection 1.3.4.

## 2.2 Validation

493 To validate the smearing functions a comparison with [25] was made where the  
 495 standard deviation, depending on the energy or momentum value of an entity,  
 496 was given, see section 2.4. To calculate this some simulated processes were needed  
 to extract data, see table 2.1.

Data	Process
Electron	$W \rightarrow e\nu$
Muon	$W \rightarrow \mu\nu$
Tau	$W \rightarrow \tau\nu$
$\gamma$	$\gamma + \text{Jet sample}$
Jets	Jet sample
$E_T^{Miss}$	$Z \rightarrow \nu\nu + \text{Jet sample}$

**Table 2.1:** Different processes from where data has been taken. Each sample is a simulation of a physical process, the simulation names can be found in appendix A

497  
 498 By plotting the data for each data point before and after the smearing function,  
 499 for that data point had been used, one can verify the functions. This is done  
 500 looking at the reco data for a given truth energy or momentum value. Since the  
 501 smearing functions take a lot of things into account the match will not be a fine  
 502 line, see figure 2.3b.

503 By fitting a Gaussian curve to this data will then result in the mean value, and  
 504 the standard deviation. The mean value is not of interest for the purposes of  
 505 the thesis, though the standard deviation is since it is this which is used in the  
 506 validation. The standard deviation is equivalent to RMS (Root mean square) and  
 507 is also known as the resolution of the data. It will from here on be denoted RMS  
 508 or  $\sigma$ .

509 This resolution is then compared to previous results, [25], and finally confirmed  
 510 or demented.

511 To get enough and thorough statistics enough data must be available for a given  
 512 truth energy or momenta and the analysis must be specific enough to only look  
 513 at a minute interval around this point.

## 514 2.3 Results

515 As discussed above, the method was to plot the data against its smeared counter-  
516 part and through this determine the RMS, ( $\sigma$ ) to see if it conforms to the expected  
517 values.

518 Since there are only slightly differences depending on pile-up these are not shown  
519 except for  $E_T^{Miss}$  and jets. Also only one energy value is shown for simplicity,  
520 though the comparison was done for different energy values.

521 Pile-up is fixed at 60 is nothing else is said used simply as a benchmark.

522 The images are, as the comparison, often divided depending on the different  $\eta$   
523 values.

524 All results are summarized in table 2.5.

### 2.3.1 Electron and photon

Since these interact very similarly in the detector, their smearing functions are identical. The slice value represents at which value of unsmeared energy or momentum this smearing occurs.

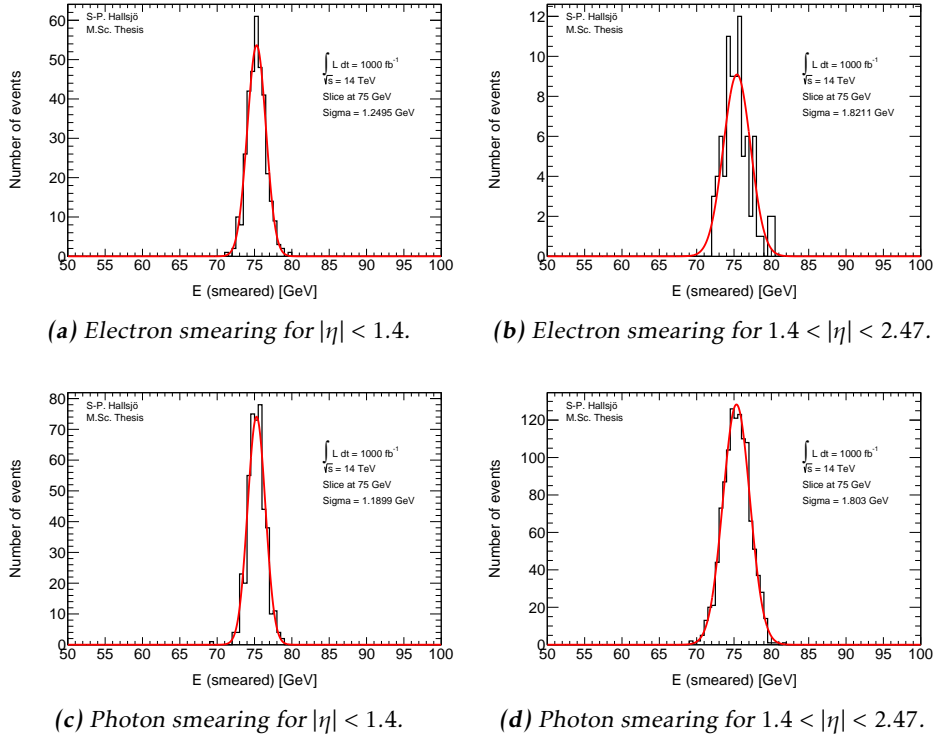


**Figure 2.1:** Photon and electron smearing plots.

529 **2.3.2 Muon**

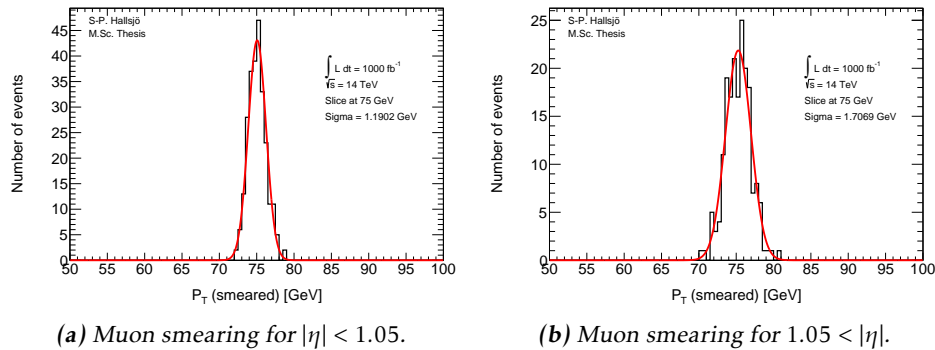


**Figure 2.2:** Muon smearing plots.

530 **2.3.3 Tau**

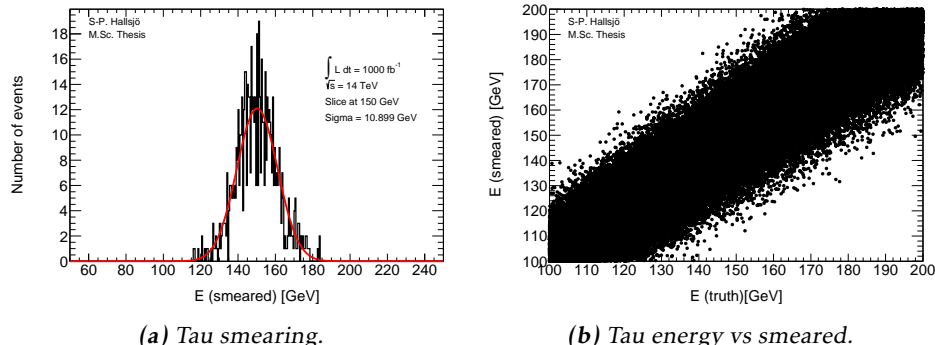


**Figure 2.3:** Tau smearing and energy vs smearing plot.

### 2.3.4 Jets

Jets as described in subsection 1.3.6, are hadronic showers. The smearing functions are divided into four different regions depending on the angle  $\eta$ .

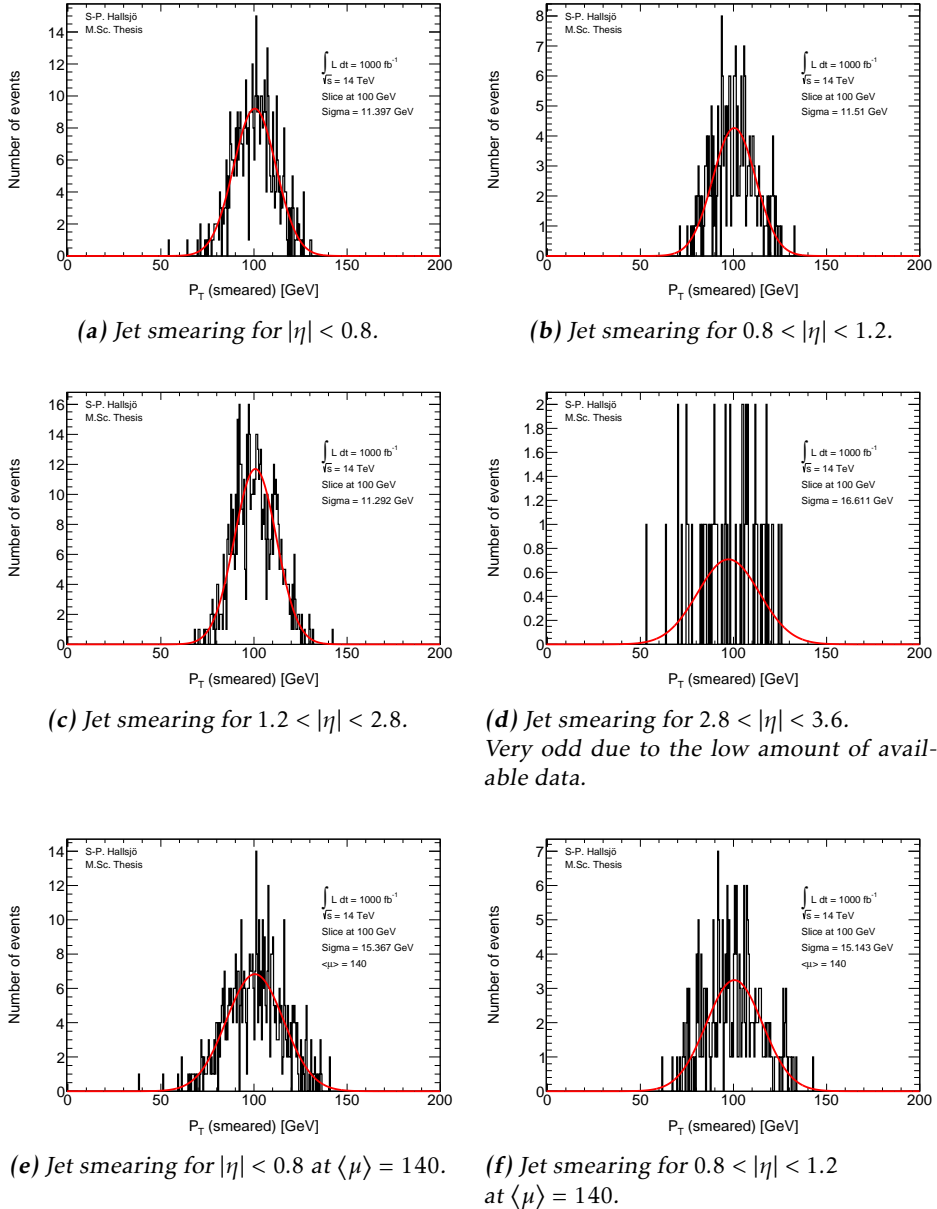


**Figure 2.4:** Jet smearing plots.

### 534 2.3.5 Missing Transversal Energy

535 These figures are given as smeared value from origin, thus at 0 it represents that  
 536 the energy is unsmeared, compared to the others where the slice value represents  
 537 the unsmeared.

538 Here the  $E_T^{Miss}$  is projected down to the x- and y-axis, since these are the transver-  
 539 sal axes, to be smeared.

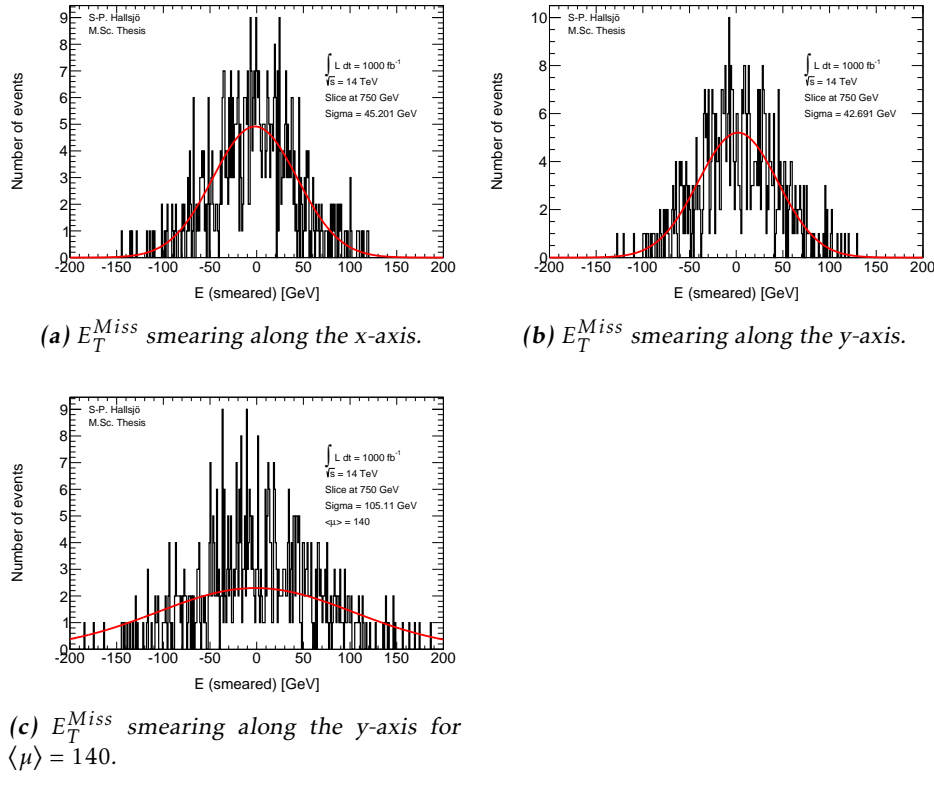


**Figure 2.5:**  $E_T^{Miss}$  smearing plots

## 2.4 Expected results

540 The expected response has been calculated and taken from [25].

541 The independence of pile-up for leptons and photons is backed up in previous  
542 research, for instance [1, 26] were the first states:

543 “The uncertainty due to pile-up was investigated by comparing  
544 simulated MC samples with and without pile-up and was found to be  
545 negligible”

546 This is also confirmed in other internal documents.

547 To validate the smearing code comparisons were made with [25] which gave the  
548 following formulation for the expected RMS:

Process	Absolute RMS
Electron & photon	$\sigma = 0.3 \oplus 0.1\sqrt{E(GeV)} \oplus 0.01E(GeV),  \eta  < 1.4$ $\sigma = 0.3 \oplus 0.15\sqrt{E(GeV)} \oplus 0.015E(GeV), 1.4 <  \eta  < 2.47$
Muon	$\sigma = \frac{\sigma_{id}\sigma_{ms}}{\sigma_{id} \oplus \sigma_{ms}}$ $\sigma_{id} = P_T(a_1 \oplus a_2 P_T)$ $\sigma_{ms} = P_T(\frac{b_0}{P_T} \oplus b_1 \oplus b_2 P_T)$
Tau	$\sigma = (0.03 \oplus \frac{0.76}{\sqrt{E(GeV)}})E(GeV)$
Jet	$\sigma = P_T(GeV)(\frac{N}{P_T} \oplus \frac{S}{\sqrt{P_T}} \oplus C)$
$E_T^{Miss}$	$\sigma = (0.4 + 0.09\sqrt{\mu})\sqrt{\sum E(GeV) + 20\mu}$

Table 2.2: Expected absolute RMS.

550 • For muon: All parameters are given in table 2.3.

551 • For tau: Fixed at 3 prong. 1 prong exists though was not used in this thesis.  
552 Where prong refers to the different amount of tracks that from which they  
553 were reconstructed.

554 • For jet: All parameters are given in table 2.4 where  $N = a(\eta) + b(\eta)\mu$ .

	$a_1$	$a_2$	$b_0$	$b_1$	$b_2$
$ \eta  < 1.05$	0.01607	0.000307	0.24	0.02676	0.00012
$ \eta  < 1.05$	0.03000	0.000307	0.00	0.03880	0.00016

Table 2.3: Parameters used in the muon smearing function take from [25].

$ \eta $	a	b	s	C
0-0.8	3.2	0.07	0.74	0.05
0.8-1.2	3.0	0.07	0.81	0.05
1.2-2.8	3.3	0.08	0.54	0.05
2.8-3.6	2.8	0.11	0.83	0.05

**Table 2.4:** Parameters used in the jet smearing function taken from [25].

Process	RMS [GeV]	Error in RMS	Expected RMS	Significance
Electron low $\eta$	1.24948	0.0481987	1.18427	1.35286
High $\eta$	1.8211	0.141329	1.74446	0.542334
Photon low $\eta$	1.18986	0.0400187	1.18427	0.139734
High $\eta$	1.80297	0.0374312	1.74446	1.56323
Muon low $\eta$	1.19016	0.0524938	1.49789	5.86235
High $\eta$	1.70694	0.0882606	2.18318	5.39575
Tau	10.8992	0.299761	10.3388	1.86975
Jet low $\eta$	11.3974	0.351391	11.5983	0.571586
$\langle \mu \rangle = 140$	15.3673	0.473783	15.7721	0.854499
Mid low $\eta$	11.5096	0.518872	11.9352	0.820407
$\langle \mu \rangle = 140$	15.1427	0.682649	15.9515	1.18475
Mid high $\eta$	11.2916	0.310314	10.9439	1.12021
High $\eta$	16.6112	1.52891	13.5	2.03491
$E_T^{Miss}$ x-axis	45.2013	1.35426	48.4483	2.39762
$E_T^{Miss}$ y-axis	42.6906	2.27904	48.4483	4.50154
$\langle \mu \rangle = 140$	105.109	12.239	87.2812	1.45667

**Table 2.5:** RMS values.

- 555 • Where the given RMS is still the absolute.  
 556 • The significance is the standard deviation of between the expected and cal-  
 557 culated with respect to the error.

## 558 2.5 Discussion

### 559 2.5.1 Smearing independent on pile-up

560 From the validation done it was interesting to note that the smearing functions  
561 were created from previous studies, [1, 26], which had shown that leptons and  
562 photons are not affected by pile-up. This may seem incredible however it be-  
563 comes quite logical when one understands how the detectors work. To be able to  
564 detect particles the detectors must detect an excess of energy which comes from  
565 a particle passing through. This should not be distorted by an increased pile-up.  
566 The amount of particles passing through will of course increase, but the detec-  
567 tions should be unaffected as well as the recreation of the events. However with  
568 the same logic it makes sense that jets and  $E_T^{Miss}$  are quite affected since they  
569 are combined of several parts, either hadronic particles or by all the transversal  
570 missing energy.

571 Another interesting part is how the effect diminishes with and increasing energy.  
572 As seen above, and through the the formula, for the high energies which were of  
573 interest here the effect is minimal.

### 574 2.5.2 Comparison to expected results

575 One of the major problems in the comparison was to get the significance of the  
576 Gaussian fit to be calculated correctly. The tool ROOT has a lot of different fea-  
577 tures which made this task somewhat difficult. Also since this is a statistical  
578 property there is a statistical fluctuation in the result.

579 Another was to retrieve the correct values from the paper, [25], since it was un-  
580 clear if the values given were absolute or scale dependent. This has now been  
581 corrected in a new version of the paper.

## 2.6 Conclusion

582 The smearing functions work as intended within 5.8 sigma, however when using  
584 a test box and averaging the sigmas one ends up with half of this for the extreme  
585 cases, muons and  $E_T^{Miss}$ y-axis.

# 3

---

## Evaluating dark matter signals

588 The main goal of the thesis is to investigate if certain dark matter signals can  
589 be detected after the high luminosity upgrade. One immediate worry is that the  
590 background will be large in comparison to the signal, making the signal undetectable.  
591

592 The following signals models have been used: The signal models are given in  
593 appendix A along with the background. The different models were discussed in  
594 part in subsection 1.2.5 and some more in this chapter.

595 Each of these has been evaluated in different signal regions and the detectability  
596 has been evaluated using a statistical P-value. This process has been performed  
597 at different pile-up values.

598 **What background existed? How was it simulated in MC? Should that be here  
599 or in appendix?**

600 Dont mention, but good to know. Used METpt in all histograms, with the weight  
601 as in main.C and mainclass.C.

### 602 3.1 Signal to background ratio

603 What I am doing now, looking at what signal? What are the different background  
604 processes? What and why was the weight used?

605 Signals should be explained somewhat in the introduction.

606 Look at presentation, is it worth bringing up the first signal regions when the  
607 data has already been filtered? Should that be here?

### 608 3.1.1 Selection criteria

609 What criteria were used and more importantly why? It is quite important that  
 610 you can explain why this was used.

611 For different purposes different selection criteria or regions are used. These are a  
 612 set of criteria specified to enhance the area of interest. For instance, if simulating  
 613 a specific signal one wants to find as many ways as possible to diminish the back-  
 614 ground. This so that when searching experimentally, the signal will be easier to  
 615 detect.

616 These can be quite general cuts, there are only some things to take into consider-  
 617 ation.

- 618 • If experimental, what limitations are set by the detectors? Are there some  
 619 criteria already?
- 620 • If simulated, is there some criteria set in the generator?
- 621 • Are there criteria which must be set since there is to much uncertainty in  
 622 the data? or a large effect of pile up?

### 623 3.1.2 Verifying background data

624 To verify that the background data was correct it was compared with [27], in  
 625 which the luminosity if  $10 \text{ fb}^{-1}$  and thus the expected values from the paper  
 626 scaled up with a factor 100. **Also, somewhat unexpectedly is that the differ-  
 627 ence in center of mass energy required the cross-sections to be much lowered  
 628 than compared with the upgrade.** The signal region used in the article were the  
 following:

---

Selection Criteria		
Jet veto, require no more than 2 jets with $p_T > 30 \text{ GeV}$ and $ \eta  < 4.5$		
Lepton veto, no electron or muon		
Leading jet with $ \eta  < 2.0$ and $\Delta\phi(\text{jet}, E_T^{\text{Miss}}) > 0.5$ (second-leading jet)		
signal region	SR3p	SR4p
minimum leading jet $p_T$ (GeV)	350	500
minimum $E_T^{\text{Miss}}$ (GeV)	350	500

---

629 *Table 3.1: The signal regions*

630 The article has several different signal regions, the difference is the last item, un-  
 631 fortunately since the simulated events are already filtered before the analysis only  
 632 one of the regions could be used.

633 NEW WITH 350 as SR3 and 500 as SR4 and expected (Scaled to  $1000 \text{ fb}^{-1}$ ) thus  
 634 scaled a factor 100 since luminosity is only a measurement of the amount of data  
 635 and does not change anything physical.

Process	SR3p	Expected SR3p	SR4p	Expected SR4p
$Z \rightarrow \nu\nu$	140298	152000	25250.3	27000
$W \rightarrow \tau\nu$	40700.8	37000	5861.74	3900
$W \rightarrow e\nu$	11229	11200	1506.58	1600
$W \rightarrow \mu\nu$	13727.1	15800	1872.32	4200
Total background	205955	218000	34491	36700

**Table 3.2:** Comparison of the simulated and expected events from [27].

636 In table 3.2 a comparison has been made. It can be seen that the simulated events  
 637 and expected events coincide on all accounts apart from  $W \rightarrow \tau\nu$ ,  $W \rightarrow \mu\nu$  and  
 638 thus the total as well. **This can be explained by better separation of  $\mu, \tau$  and**  
 639 **missing energy.** Tau can not be reconstructed as jets in the code, they can in  
 640 reality!

### 641 3.1.3 Figures of merit

642 **P-value, info from Majas phd thesis. Is there a source? Should there be a fig-**  
 643 **ure?**

644 To be able to evaluate different signal regions and different signal models, a figure  
 645 of merit  $p$  is used. The value  $p$  is the probability for an assumed hypothesis  
 646 to be correct, thus a good signal region will yield a low value. The assumed  
 647 hypothesis is that the background and its fluctuations is measured over the signal  
 648 plus background.

649 Assuming the expected number of background events are  $B \pm \sigma_B$  where  $\sigma_B$  is the  
 650 quadratic sum of the statistical error from Monte Carlo, the statistical error from  
 651 the control region and the systematic errors. The expected number of signals is  $S$ ,  
 652 assumed without fluctuation.

653 If no uncertainty in  $B$  or  $S$  is assumed, then the number of expected events,  $N$ , in  
 654 the signal region should follow a Poisson distribution as such:

$$P(N|S+B) = \frac{e^{-(S+B)}(S+B)^N}{N!} \quad (3.1)$$

655 However since there is an uncertainty in the background, the probability distri-  
 656 bution  $P(N|S+B)$  must be convoluted with a Gaussian function:

$$G(N_B|B, \sigma_B) = \frac{1}{\sigma_B \sqrt{2\pi}} e^{-\frac{(N_B - B)^2}{2\sigma_B^2}} \quad (3.2)$$

where  $N_B$  is the expected number of background events. The convolution is done

using  $N_B$  as  $N$  resulting in the total probability density function:

$$\begin{aligned} F(N|S+B, \sigma_B) &= P(N|S+N_B)*G(N_B|B, \sigma_B) = \\ &= \int_{-\infty}^{\infty} P(N|N_B - (S + B))G(N_B|B, \sigma_B)dN_B \end{aligned} \quad (3.3)$$

657 This leads to the probability of the signal plus background fluctuation to B events  
 658 being obtained by summing the probability function from  $N=0$  to  $N=B$ .

$$p = \sum_{i=0}^B \int_{-\infty}^{\infty} P(i|N_B - (S+B))G(N_B|B, \sigma_B)dN_B \quad (3.4)$$

### 659 3.1.4 D5 operators

660 Discuss  $M^*$ , and the difference in mDM. From presentation given, 3-4 April.  
 661 Was discussed in part in subsection 1.2.5  
 662 As described in the introduction **reference?**, one of the signals is modelled using  
 663 the D5 operator. In this thesis two different scenarios were used, one at a dark  
 664 matter mass of 50 GeV and one at 400 GeV.

### 665 3.1.5 Light vector mediator models

666 Discuss  $M_m$ , width, and the difference in mDM. From presentation given, 3-4  
 667 April.  
 668 Was discussed in part in subsection 1.2.5  
 669 As described in the introduction **reference?**, the other signal model is a vector  
 670 mediator model. The data available is: two different widths  $M/3$  and  $M/8\pi$ .  
 671 **M?!**? two different mDM, 50 GeV and 400 GeV and finally a variety of mediator  
 672 masses.

### 673 3.1.6 Susy models?

## 674 3.2 Other selection criteria and observables

675 New signal regions.

## 676 3.3 Mitigating the effect of the high luminosity

677 Something pile-up Something as seen in validation of... the effect is quite minute  
 678 for high energy values and does not at all affect leptons or photons. Mention that  
 679 the effect is on a trigger level, that the lowest SR will be lost.

680 Even though this was envisioned as the primary focus of the thesis, it was shown  
 681 that the effect of pile-up is minute for these high signal regions. Thus the focus

---

**Selection Criteria**


---

Jet veto, require no more than 2 jets with  $p_T > 30\text{GeV}$  and  $|\eta| < 4.5$

Lepton veto, no electron or muon

Leading jet with  $|\eta| < 2.0$  and  $\Delta\phi(\text{jet}, E_T^{\text{Miss}}) > 0.5$  (second-leading jet)

signal region	SR0	SR1	SR2	SR3	SR4
minimum leading jet $p_T$ (GeV)	120	350	600	800	1000
minimum $E_T^{\text{Miss}}$ (GeV)	120	350	600	800	1000
signal region	SR0	SRa	SRb	SRc	SRd
minimum leading jet $p_T$ (GeV)	350	350	350	350	350
minimum $E_T^{\text{Miss}}$ (GeV)	120	350	600	800	1000

**Table 3.3:** The new signal regions

682 was shifted to perform a more in-depth mono-jet analysis of different DM signal  
683 models.

## 684 3.4 Results

### 685 3.4.1 Limit on $M^*$

686 The mass suppression scale. Give at  $1000\text{fb}^{-1}$ . And for the different signal re-  
687 gions. **ASK CHRISTOPHE FOR A GOOD EXPLANATION OF  $M^*$  and why**  
688 **there can be limits!**

689 For the new signal regions: **Include a table of the limits for truth and Reco.**

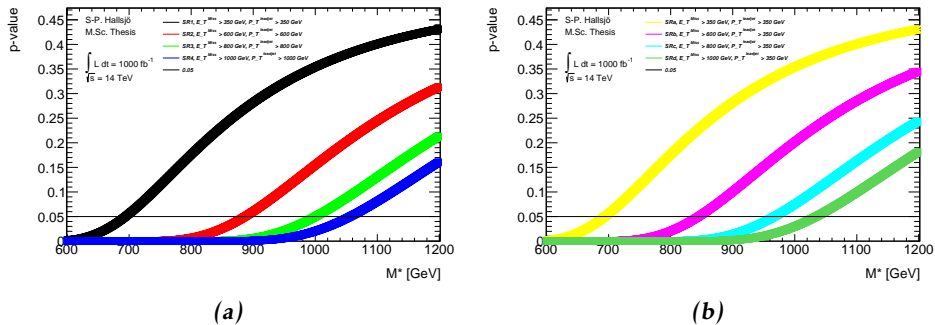


**Figure 3.1:** On a truth level.

### 690 3.4.2 Effect of pile-up on $M^*$

691 Hardly any effect. 10 % or in that vicinity.

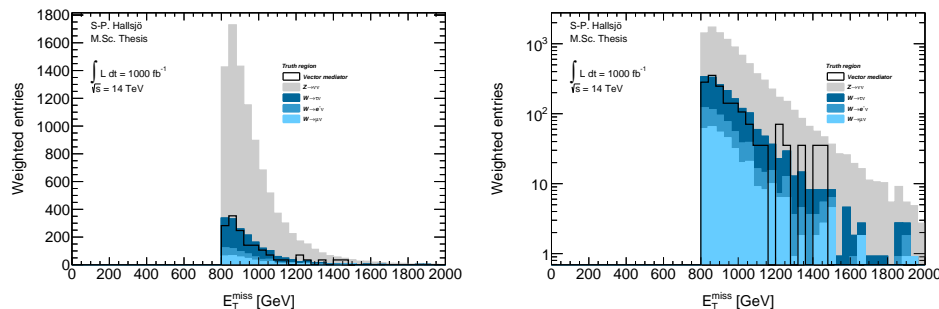
### 692 3.4.3 Previous results

693 Valerios paper for instance. Preliminary note that much better results for 1000fb-1  
 694 and 14TeV.

695 The whole discussion with Steven and David.

### 696 3.4.4 Limit on mediator mass

697 Are there previous results? Signal vs background plot in normal and log scale for  
 698 one of the vector mediator models, to be able to evaluate all the different models  
 699 the so called p-value was used in different signal regions. Below are two figures  
 700 showing one of the vector mediator models in SR3.



(a) Signal on background plot for  $E_T^{Miss}$  on reco level in SR3. (b) The same as a) with log scale on the y-axis

**Figure 3.2:** Signal on background plot to illustrate the a general plot.

701 To set a limit on the mediator mass the p-value was calculated in different sig-  
 702 nals regions for the different signal models with different mediator mass. This  
 703 resulted in the following plot:

### 704 3.4.5 Effect of pile-up on mediator mass

705 Check the different cases for reco and truth to see what happens.

## 706 3.5 Discussion

## 707 3.6 Conclusion

# 4

---

## Results and Conclusions

710 **4.1 Validation of smearing functions**

711 Have some discussion.

712 Result they appear to work as expected, the reference paper was a bit unclear, I  
713 leave my writing as a better reference.

714 **4.2 Signal to background ratio**

715 **4.2.1 Limit on  $M^*$**

716 **4.2.2 Limit on mediator mass**

717 **4.3 Other selection criteria and observables**

718 **4.3.1 Limit on  $M^*$**

719 **4.3.2 Limit on mediator mass**

720 **4.4 Mitigating the effect of the high luminosity**

721 **4.5 Recommendations to mitigate the effect of the  
722 high luminosity**

723 Keep to a higher energy region, or signal region.

## 724 4.6 Suggestions for future research

725 With more time, search for new signal regions, the only solution now for the HL  
726 is to go up in energy. Since none of the other parameters (eta,phi etc) seem to be  
727 altered these can not be used. Is there something that has been overlooked?

728 Test the effect of pile-up for lower signal regions? See if the effect is as great as  
729 predicted.

730 Explore other theoretical models for dark matter, other d operators etc. Models  
731 that are based on Supersymmetry and not just effective theories.

732 Sätt av ett kort kapitel sist i rapporten till att avrunda och föreslå räkningar för  
733 framtida utveckling av arbetet.

734 Saving as reference. test citing as: Here we cite Duck [28] [28].

735 If the above works, remember to edit myreferences.

# Appendix



737

# A

738

---

## Datasets

### 739 A.1 Background processes

#### 740 A.1.1 Validation

741 For the validation the following datasets were used, with a filter at generator level  
742 at 450GeV for lead jet and MET.

743 mc12.157539.sherpa\_ct10\_znunupt280d4pd.v03 mc12.157534.sherpa\_ct10\_  
744 wenupt200d4pd.v03

745 mc12.157535.sherpa\_ct10\_wmunupt200d4pd.v03

746 mc12.157536.sherpa\_ct10\_wtaunupt200d4pd.v03

747 mc12.129160.pythia8\_au2cteq6l1\_perf\_jf17d4pd.v03

748 mc12.129160.pythia8\_au2cteq6l1\_perf\_jf17d4pd.v04

749 mc12.129170.pythia8\_au2cteq6l1\_gammajet\_dp17d4pd.v04

750 They should be read as such: Monte Carlo version, dataset number, generator, ?  
751 name.

#### 752 A.1.2 Background to signals

753 The same as the above though now with the filter as indicated by their name. The  
754 second znunu sample has been generated with and center of mass energy at 8  
755 TeV.

756 mc12.157539.sherpa\_ct10\_znunupt280d4pd.v05

757 mc12.157539.8tev\_sherpa\_ct10\_znunupt280d4pd.v05

758 mc12.157536.sherpa\_ct10\_wtaunupt200d4pd.v05

759 mc12.157534.sherpa\_ct10\_wenupt200d4pd.v05

760 mc12.157535.sherpa\_ct10\_wmunupt200d4pd.v05

## 761 A.2 D5 signal processes

```

762 mc12.188408.madgraphpythia_auet2bcteq6l1_d5_dm50_ms10000_
763 qcut200d4pd.v06
764 mc12.188409.madgraphpythia_auet2bcteq6l1_d5_dm50_ms10000_
765 qcut400d4pd.v06
766 mc12.188410.madgraphpythia_auet2bcteq6l1_d5_dm50_ms10000_
767 qcut600d4pd.v06

768 mc12.188411.madgraphpythia_auet2bcteq6l1_d5_dm400_ms10000_
769 qcut200d4pd.v06
770 mc12.188412.madgraphpythia_auet2bcteq6l1_d5_dm400_ms10000_
771 qcut400d4pd.v06
772 mc12.188413.madgraphpythia_auet2bcteq6l1_d5_dm400_ms10000_
773 qcut600d4pd.v06

774 All signals should be read as such: Monte Carlo version, dataset number, genera-
775 tor, ?, name of operator, dark matter mass, default mass suppression scale,
776 qcut part. As discussed in reference
777 qcut means that the original data has been split into different parts depending on
778 the value of the lead jet pt.

```

## 779 A.3 Light vector mediator processes

```

780 mc12.188414.madgraphpythia_auet2bcteq6l1_dmv_dm50_mm100_w3_
781 qcut200d4pd.v06
782 mc12.188422.madgraphpythia_auet2bcteq6l1_dmv_dm50_mm100_w3_
783 qcut400d4pd.v06
784 mc12.188430.madgraphpythia_auet2bcteq6l1_dmv_dm50_mm100_w3_
785 qcut600d4pd.v06

786 mc12.188415.madgraphpythia_auet2bcteq6l1_dmv_dm50_mm300_w3_
787 qcut200d4pd.v06
788 mc12.188423.madgraphpythia_auet2bcteq6l1_dmv_dm50_mm300_w3_
789 qcut400d4pd.v06
790 mc12.188431.madgraphpythia_auet2bcteq6l1_dmv_dm50_mm300_w3_
791 qcut600d4pd.v06

792 mc12.188416.madgraphpythia_auet2bcteq6l1_dmv_dm50_mm500_w3_
793 qcut200d4pd.v06
794 mc12.188424.madgraphpythia_auet2bcteq6l1_dmv_dm50_mm500_w3_
795 qcut400d4pd.v06
796 mc12.188432.madgraphpythia_auet2bcteq6l1_dmv_dm50_mm500_w3_
797 qcut600d4pd.v06

798 mc12.188417.madgraphpythia_auet2bcteq6l1_dmv_dm50_mm1000_w3_
799 qcut200d4pd.v06
800 mc12.188425.madgraphpythia_auet2bcteq6l1_dmv_dm50_mm1000_w3_

```

```
801 qcut400d4pd.v06
802 mc12.188433.madgraphpythia_auet2bcteq6l1_dmv_dm50_mm1000_w3_
803 qcut600d4pd.v06
804 mc12.188418.madgraphpythia_auet2bcteq6l1_dmv_dm50_mm3000_w3_
805 qcut200d4pd.v06
806 mc12.188426.madgraphpythia_auet2bcteq6l1_dmv_dm50_mm3000_w3_
807 qcut400d4pd.v06
808 mc12.188434.madgraphpythia_auet2bcteq6l1_dmv_dm50_mm3000_w3_
809 qcut600d4pd.v06
810 mc12.188419.madgraphpythia_auet2bcteq6l1_dmv_dm50_mm6000_w3_
811 qcut200d4pd.v06
812 mc12.188427.madgraphpythia_auet2bcteq6l1_dmv_dm50_mm6000_w3_
813 qcut400d4pd.v06
814 mc12.188435.madgraphpythia_auet2bcteq6l1_dmv_dm50_mm6000_w3_
815 qcut600d4pd.v06
816 mc12.188420.madgraphpythia_auet2bcteq6l1_dmv_dm50_mm10000_w3_
817 qcut200d4pd.v06
818 mc12.188428.madgraphpythia_auet2bcteq6l1_dmv_dm50_mm10000_w3_
819 qcut400d4pd.v06
820 mc12.188436.madgraphpythia_auet2bcteq6l1_dmv_dm50_mm10000_w3_
821 qcut600d4pd.v06
822 mc12.188421.madgraphpythia_auet2bcteq6l1_dmv_dm50_mm15000_w3_
823 qcut200d4pd.v06
824 mc12.188429.madgraphpythia_auet2bcteq6l1_dmv_dm50_mm15000_w3_
825 qcut400d4pd.v06
826 mc12.188437.madgraphpythia_auet2bcteq6l1_dmv_dm50_mm15000_w3_
827 qcut600d4pd.v06
828 mc12.188438.madgraphpythia_auet2bcteq6l1_dmv_dm50_mm100_w8pi_
829 qcut200d4pd.v06
830 mc12.188446.madgraphpythia_auet2bcteq6l1_dmv_dm50_mm100_w8pi_
831 qcut400d4pd.v06
832 mc12.188454.madgraphpythia_auet2bcteq6l1_dmv_dm50_mm100_w8pi_
833 qcut600d4pd.v06
834 mc12.188439.madgraphpythia_auet2bcteq6l1_dmv_dm50_mm300_w8pi_
835 qcut200d4pd.v06
836 mc12.188447.madgraphpythia_auet2bcteq6l1_dmv_dm50_mm300_w8pi_
837 qcut400d4pd.v06
838 mc12.188455.madgraphpythia_auet2bcteq6l1_dmv_dm50_mm300_w8pi_
839 qcut600d4pd.v06
840 mc12.188440.madgraphpythia_auet2bcteq6l1_dmv_dm50_mm500_w8pi_
841 qcut200d4pd.v06
842 mc12.188448.madgraphpythia_auet2bcteq6l1_dmv_dm50_mm500_w8pi_
```

```
843 qcut400d4pd.v06
844 mc12.188456.madgraphpythia_auet2bcteq6l1_dmv_dm50_mm500_w8pi_
845 qcut600d4pd.v06

846 mc12.188441.madgraphpythia_auet2bcteq6l1_dmv_dm50_mm1000_w8pi_
847 qcut200d4pd.v06
848 mc12.188449.madgraphpythia_auet2bcteq6l1_dmv_dm50_mm1000_w8pi_
849 qcut400d4pd.v06
850 mc12.188457.madgraphpythia_auet2bcteq6l1_dmv_dm50_mm1000_w8pi_
851 qcut600d4pd.v06

852 mc12.188442.madgraphpythia_auet2bcteq6l1_dmv_dm50_mm3000_w8pi_
853 qcut200d4pd.v06
854 mc12.188450.madgraphpythia_auet2bcteq6l1_dmv_dm50_mm3000_w8pi_
855 qcut400d4pd.v06
856 mc12.188458.madgraphpythia_auet2bcteq6l1_dmv_dm50_mm3000_w8pi_
857 qcut600d4pd.v06

858 mc12.188444.madgraphpythia_auet2bcteq6l1_dmv_dm50_mm10000_w8pi_
859 qcut200d4pd.v06
860 mc12.188452.madgraphpythia_auet2bcteq6l1_dmv_dm50_mm10000_w8pi_
861 qcut400d4pd.v06
862 mc12.188460.madgraphpythia_auet2bcteq6l1_dmv_dm50_mm10000_w8pi_
863 qcut600d4pd.v06

864 mc12.188445.madgraphpythia_auet2bcteq6l1_dmv_dm50_mm15000_w8pi_
865 qcut200d4pd.v06
866 mc12.188453.madgraphpythia_auet2bcteq6l1_dmv_dm50_mm15000_w8pi_
867 qcut400d4pd.v06
868 mc12.188461.madgraphpythia_auet2bcteq6l1_dmv_dm50_mm15000_w8pi_
869 qcut600d4pd.v06

870 mc12.188462.madgraphpythia_auet2bcteq6l1_dmv_dm400_mm500_w3_
871 qcut200d4pd.v06
872 mc12.188468.madgraphpythia_auet2bcteq6l1_dmv_dm400_mm500_w3_
873 qcut400d4pd.v06
874 mc12.188474.madgraphpythia_auet2bcteq6l1_dmv_dm400_mm500_w3_
875 qcut600d4pd.v06

876 mc12.188463.madgraphpythia_auet2bcteq6l1_dmv_dm400_mm1000_w3_
877 qcut200d4pd.v06
878 mc12.188469.madgraphpythia_auet2bcteq6l1_dmv_dm400_mm1000_w3_
879 qcut400d4pd.v06
880 mc12.188475.madgraphpythia_auet2bcteq6l1_dmv_dm400_mm1000_w3_
881 qcut600d4pd.v06

882 mc12.188464.madgraphpythia_auet2bcteq6l1_dmv_dm400_mm3000_w3_
883 qcut200d4pd.v06
884 mc12.188470.madgraphpythia_auet2bcteq6l1_dmv_dm400_mm3000_w3_
```

```
885 qcut400d4pd.v06
886 mc12.188476.madgraphpythia_auet2bcteq6l1_dmv_dm400_mm3000_w3_
887 qcut600d4pd.v06
888 mc12.188465.madgraphpythia_auet2bcteq6l1_dmv_dm400_mm6000_w3_
889 qcut200d4pd.v06
890 mc12.188471.madgraphpythia_auet2bcteq6l1_dmv_dm400_mm6000_w3_
891 qcut400d4pd.v06
892 mc12.188477.madgraphpythia_auet2bcteq6l1_dmv_dm400_mm6000_w3_
893 qcut600d4pd.v06
894 mc12.188466.madgraphpythia_auet2bcteq6l1_dmv_dm400_mm10000_w3_
895 qcut200d4pd.v06
896 mc12.188472.madgraphpythia_auet2bcteq6l1_dmv_dm400_mm10000_w3_
897 qcut400d4pd.v06
898 mc12.188478.madgraphpythia_auet2bcteq6l1_dmv_dm400_mm10000_w3_
899 qcut600d4pd.v06
900 mc12.188467.madgraphpythia_auet2bcteq6l1_dmv_dm400_mm15000_w3_
901 qcut200d4pd.v06
902 mc12.188473.madgraphpythia_auet2bcteq6l1_dmv_dm400_mm15000_w3_
903 qcut400d4pd.v06
904 mc12.188479.madgraphpythia_auet2bcteq6l1_dmv_dm400_mm15000_w3_
905 qcut600d4pd.v06
906 mc12.188480.madgraphpythia_auet2bcteq6l1_dmv_dm400_mm500_w8pi_
907 qcut200d4pd.v06
908 mc12.188486.madgraphpythia_auet2bcteq6l1_dmv_dm400_mm500_w8pi_
909 qcut400d4pd.v06
910 mc12.188492.madgraphpythia_auet2bcteq6l1_dmv_dm400_mm500_w8pi_
911 qcut600d4pd.v06
912 mc12.188481.madgraphpythia_auet2bcteq6l1_dmv_dm400_mm1000_w8pi_
913 qcut200d4pd.v06
914 mc12.188487.madgraphpythia_auet2bcteq6l1_dmv_dm400_mm1000_w8pi_
915 qcut400d4pd.v06
916 mc12.188493.madgraphpythia_auet2bcteq6l1_dmv_dm400_mm1000_w8pi_
917 qcut600d4pd.v06
918 mc12.188482.madgraphpythia_auet2bcteq6l1_dmv_dm400_mm3000_w8pi_
919 qcut200d4pd.v06
920 mc12.188488.madgraphpythia_auet2bcteq6l1_dmv_dm400_mm3000_w8pi_
921 qcut400d4pd.v06
922 mc12.188494.madgraphpythia_auet2bcteq6l1_dmv_dm400_mm3000_w8pi_
923 qcut600d4pd.v06
924 mc12.188483.madgraphpythia_auet2bcteq6l1_dmv_dm400_mm6000_w8pi_
925 qcut200d4pd.v06
926 mc12.188489.madgraphpythia_auet2bcteq6l1_dmv_dm400_mm6000_w8pi_
```

```
927 qcut400d4pd.v06
928 mc12.188495.madgraphpythia_auet2bcteq6l1_dmv_dm400_mm6000_w8pi_
929 qcut600d4pd.v06
930 mc12.188484.madgraphpythia_auet2bcteq6l1_dmv_dm400_mm10000_w8pi_
931 qcut200d4pd.v06
932 mc12.188490.madgraphpythia_auet2bcteq6l1_dmv_dm400_mm10000_w8pi_
933 qcut400d4pd.v06
934 mc12.188496.madgraphpythia_auet2bcteq6l1_dmv_dm400_mm10000_w8pi_
935 qcut600d4pd.v06
936 mc12.188485.madgraphpythia_auet2bcteq6l1_dmv_dm400_mm15000_w8pi_
937 qcut200d4pd.v06
938 mc12.188491.madgraphpythia_auet2bcteq6l1_dmv_dm400_mm15000_w8pi_
939 qcut400d4pd.v06
940 mc12.188497.madgraphpythia_auet2bcteq6l1_dmv_dm400_mm15000_w8pi_
941 qcut600d4pd.v06
```

942

943

---

## Bibliography

- [1] Collaboration ATLAS. Letter of Intent for the Phase-II Upgrade of the ATLAS Experiment. Dec 2012. URL <https://cds.cern.ch/record/1502664/>. Cited on pages 1, 17, 25, and 27.
- [2] B.H. Bransden and C.J. Joachain. *Quantum mechanics*. Pearson Education, second edition, 2000. Cited on page 3.
- [3] Sven-Patrik Hallsjö. Covering the sphere with noncontextuality inequalities. Bachelor's thesis, Linköping University, The Institute of Technology, 2013. URL [http://urn.kb.se/resolve?urn=urn:nbn:se:liu:diva-103663](http://urn.kb.se/resolve?urn=urn:nbn:se:liu.diva-103663). Cited on page 3.
- [4] A. Zee. *Quantum Field Theory in a Nutshell*. Princeton University Press, illustrated edition edition, March 2003. ISBN 0691010196. Cited on pages 3, 6, and 7.
- [5] Herbert Goldstein, Charles P. Poole, and John L. Safko. *Classical Mechanics (3rd Edition)*. Addison-Wesley, 3 edition, June 2001. ISBN 0201657023. Cited on page 3.
- [6] W. E. Burcham and M. Jobes. *Nuclear and Particle Physics*. Pearson education, second edition, 1995. Cited on page 4.
- [7] The ATLAS Collaboration. Observation of a new particle in the search for the Standard Model Higgs boson with the ATLAS detector at the LHC. *Phys. Lett. B*, 716(arXiv:1207.7214). CERN-PH-EP-2012-218):1–29. 39 p, Aug 2012. Cited on page 4.
- [8] Standard model of elementary particles. [http://en.wikipedia.org/wiki/File:Standard\\_Model\\_of\\_Elementary\\_Particles.svg](http://en.wikipedia.org/wiki/File:Standard_Model_of_Elementary_Particles.svg), 2014. Accessed: 2014-03-24. Cited on page 4.
- [9] G. Jungman, M. Kamionkowski, and K. Griest. Supersymmetric dark matter. *Physics Reports*, 267:195–373, March 1996. doi: 10.1016/0370-1573(95)00058-5. Cited on pages 4 and 5.

- 971 [10] NASA. NASA's solar system exploration: the planets: orbits and  
972 physical characteristics. [https://solarsystem.nasa.gov/planets/](https://solarsystem.nasa.gov/planets/charchart.cfm)  
973 charchart.cfm, 2014. Accessed: 2014-03-21. Cited on page 6.
- 974 [11] T. S. van Albada, J. N. Bahcall, K. Begeman, and R. Sancisi. Distribution  
975 of dark matter in the spiral galaxy NGC 3198. *Astrophysical Journal*, 295:  
976 305–313, August 1985. doi: 10.1086/163375. Cited on page 6.
- 977 [12] Jessica Goodman, Masahiro Ibe, Arvind Rajaraman, William Shepherd,  
978 Tim M.P. Tait, et al. Constraints on Light Majorana dark Matter from Colliders.  
979 *Phys.Lett.*, B695:185–188, 2011. doi: 10.1016/j.physletb.2010.11.009.  
980 Cited on pages 5 and 7.
- 981 [13] ATLAS Collaboration. Search for dark matter candidates and large extra di-  
982 mensions in events with a jet and missing transverse momentum with the at-  
983 las detector. *J. High Energy Phys.*, 04(arXiv:1210.4491. CERN-PH-EP-2012-  
984 210):075. 58 p, October 2012. URL [http://cds.cern.ch/record/](http://cds.cern.ch/record/1485031)  
985 1485031. Cited on pages 5, 8, and 9.
- 986 [14] J. Goodman, M. Ibe, A. Rajaraman, W. Shepherd, T. M. P. Tait, and H.-B. Yu.  
987 Constraints on dark matter from colliders. *Phys.Rev.D82:116010,2010*, 82  
988 (11):116010, December 2010. doi: 10.1103/PhysRevD.82.116010. Cited on  
989 page 7.
- 990 [15] ATLAS. Atlas luminosity public results. <https://twiki.cern.ch/twiki/bin/view/AtlasPublic/LuminosityPublicResults>, 2013.  
991 Accessed: 2014-03-06. Cited on page 10.
- 992 [16] AC Team. The four main LHC experiments, Jun 1999. URL <http://cds.cern.ch/record/40525>. Cited on page 10.
- 993 [17] Werner Herr and B Muratori. Concept of luminosity. 2006. URL <http://cds.cern.ch/record/941318/>. Cited on page 11.
- 994 [18] The ATLAS Collaboration. The atlas experiment at the cern large hadron col-  
995 linder. *Journal of Instrumentation*, 3(08):S08003. 437 p, 2008. URL <https://cdsweb.cern.ch/record/1129811/>. Cited on pages 11 and 12.
- 996 [19] Joao Pequenao. Computer generated image of the whole ATLAS detector,  
997 Mar 2008. URL <http://cds.cern.ch/record/1095924>. Cited on page  
998 12.
- 999 [20] ATLAS Collaboration. Event display for one of the monojet candidates in  
1000 the data. The event has a jet with  $\text{pt} = 602 \text{ GeV}$  at  $\eta = -1$  and  $\phi =$   
1001  $2.6$ ,  $\text{MET} = 523 \text{ GeV}$ , and no additional jet with  $\text{pt}_{\text{jet}} > 30 \text{ GeV}$  in the fi-  
1002 nal state.. [https://atlas.web.cern.ch/Atlas/GROUPS/PHYSICS/](https://atlas.web.cern.ch/Atlas/GROUPS/PHYSICS/CONFNOTES/ATLAS-CONF-2011-096/fig_08.png)  
1003 CONFNOTES/ATLAS-CONF-2011-096/fig\_08.png, 2011. Accessed:  
1004 2014-03-28. Cited on page 13.
- 1005 [21] ATLAS Collaboration. Physics at a High-Luminosity LHC with ATLAS. Jul  
1006

- 1010            2013. URL <https://cds.cern.ch/record/1564937>. Cited on page  
1011            15.
- 1012 [22] J. Alwall, M. Herquet, F. Maltoni, O. Mattelaer, and T. Stelzer. MadGraph  
1013            5: going beyond. *Journal of High Energy Physics*, 6:128, June 2011. doi:  
1014            10.1007/JHEP06(2011)128. Cited on page 15.
- 1015 [23] Torbjörn Sjöstrand, Stephen Mrenna, and Peter Skands. A brief introduc-  
1016            tion to {PYTHIA} 8.1. *Computer Physics Communications*, 178(11):852 –  
1017            867, 2008. ISSN 0010-4655. doi: [http://dx.doi.org/10.1016/j.cpc.2008.  
1018            01.036](http://dx.doi.org/10.1016/j.cpc.2008.01.036). URL [http://www.sciencedirect.com/science/article/  
1019            pii/S0010465508000441](http://www.sciencedirect.com/science/article/pii/S0010465508000441). Cited on page 15.
- 1020 [24] The ROOT Team. Root. <http://root.cern.ch/drupal/>, 2014. Ac-  
1021            cessed: 2014-03-28. Cited on page 15.
- 1022 [25] ATLAS Collaboration. Performance assumptions for an upgraded ATLAS  
1023            detector at a High-Luminosity LHC. Mar 2013. URL [https://cds.cern.  
1024            ch/record/1527529/](https://cds.cern.ch/record/1527529/). Cited on pages 17, 19, 25, 26, and 27.
- 1025 [26] ATLAS Collaboration. Electron performance measurements with the ATLAS  
1026            detector using the 2010 LHC proton-proton collision data. *Eur. Phys. J. C*,  
1027            72(arXiv:1110.3174. CERN-PH-EP-2011-117):1909. 45 p, Oct 2011. Com-  
1028            ments: 33 pages plus author list (45 pages total), 24 figures, 12 tables, sub-  
1029            mitted to Eur. Phys. J. C. Cited on pages 25 and 27.
- 1030 [27] ATLAS Collaboration. Search for New Phenomena in Monojet plus Missing  
1031            Transverse Momentum Final States using 10fb-1 of pp Collisions at  $\sqrt{s}=8$   
1032            TeV with the ATLAS detector at the LHC. Nov 2012. URL <http://cds.cern.ch/record/1493486/>. Cited on pages 30 and 31.
- 1033 [28] Donald Duck. The history of automatic control. *Duckburg Journal of Sci-  
1034            ence*, 106(3):345–401, 2005. Cited on page 36.
- 1035



## 1037 Upphovsrätt

1038 Detta dokument hålls tillgängligt på Internet — eller dess framtida ersättare —  
 1039 under 25 år från publiceringsdatum under förutsättning att inga extraordinära  
 1040 omständigheter uppstår.

1041 Tillgång till dokumentet innebär tillstånd för var och en att läsa, ladda ner,  
 1042 skriva ut enstaka kopior för enskilt bruk och att använda det oförändrat för icke-  
 1043 kommersiell forskning och för undervisning. Överföring av upphovsrätten vid  
 1044 en senare tidpunkt kan inte upphäva detta tillstånd. All annan användning av  
 1045 dokumentet kräver upphovsmannens medgivande. För att garantera äktheten,  
 1046 säkerheten och tillgängligheten finns det lösningar av teknisk och administrativ  
 1047 art.

1048 Upphovsmannens ideella rätt innehåller rätt att bli nämnd som upphovsman  
 1049 i den omfattning som god sed kräver vid användning av dokumentet på ovan  
 1050 beskrivna sätt samt skydd mot att dokumentet ändras eller presenteras i sådan  
 1051 form eller i sådant sammanhang som är kränkande för upphovsmannens litterära  
 1052 eller konstnärliga anseende eller egenart.

1053 För ytterligare information om Linköping University Electronic Press se för-  
 1054 lagets hemsida <http://www.ep.liu.se/>

## 1055 Copyright

1056 The publishers will keep this document online on the Internet — or its possi-  
 1057 ble replacement — for a period of 25 years from the date of publication barring  
 1058 exceptional circumstances.

1059 The online availability of the document implies a permanent permission for  
 1060 anyone to read, to download, to print out single copies for his/her own use and  
 1061 to use it unchanged for any non-commercial research and educational purpose.  
 1062 Subsequent transfers of copyright cannot revoke this permission. All other uses  
 1063 of the document are conditional on the consent of the copyright owner. The  
 1064 publisher has taken technical and administrative measures to assure authenticity,  
 1065 security and accessibility.

1066 According to intellectual property law the author has the right to be men-  
 1067 tioned when his/her work is accessed as described above and to be protected  
 1068 against infringement.

1069 For additional information about the Linköping University Electronic Press  
 1070 and its procedures for publication and for assurance of document integrity, please  
 1071 refer to its www home page: <http://www.ep.liu.se/>